MANF, ER STRESS AND THE PATHOPHYSIOLOGY OF PARKINSON'S DISEASE

MESENCEPHALIC ASTROCYTE-DERIVED NEUROTROPHIC FACTOR, ER STRESS AND THE PATHOPHYSIOLOGY OF NEURODEGENERATIVE DISORDERS

By KHALED NAWAR, H.B.Sc 001425813

Principle Investigator: Dr. Ram K. Mishra

Thesis Report Submitted to the School of Graduate Studies in Partial Fulfilment of the Requirements for the Degree Master of Science

Neuroscience Graduate Program
McMaster University

Name:	Khaled Nawar
Degree:	Master of Science
Title:	MESENCEPHALIC ASTROCYTE-DERIVED NEUROTROPHIC FACTOR, ER STRESS AND THE PATHOPHYSIOLOGY OF NEURODEGENERATIVE DISORDERS
Examining Committee:	**Dr. Ram K. Mishra** Senior Supervisor
	Dr. Bhagwati Gupta Committee member
	Dr. Benicio Frey Committee member

Number of pages: 78

McMaster UNIVERSITY

July 2019

ABSTRACT

Nearly 10 million people worldwide live with Parkinson's Disease (PD), a disease marked by the degeneration of midbrain dopaminergic neurons. Current treatments are symptomatic and can incur undesirable side effects. The recently discovered neurotrophic factor (NTF), known as mesencephalic astrocyte-derived neurotrophic factor (MANF), has proven to be an interesting candidate to study within the context of PD because this NTF is involved in endoplasmic reticulum (ER) homeostasis and the unfolded protein response (UPR), both of which are abnormal in PD. MANF is an evolutionary conserved NTF identified in both invertebrate and vertebrate species that is mainly localized within the ER and has demonstrated to be neuroprotective against midbrain DA neuron degeneration in vitro. Intracellular MANF helps stop the unfolded protein response (UPR) during ER stress, and therefore prevents the cell from going into apoptosis. Lentiviral mediated shRNA knockdown of MANF in rats has led to the manifestation of PD like symptoms and motor deficits mainly due to the death of dopaminergic neurons in the substantia nigra (SN). mRNA analysis of the ER stress marker glucose-regulated protein 78 (GRP78) and the transcription factor C/EBP homologous protein (CHOP) have shown increased levels apoptosis following MANF knockdown. Furthermore, the phytochemical curcumin is a spice that has been widely acknowledged for its anti-oxidant and anti-apoptotic properties and in-vitro investigation of its protective role has revealed that curcumin prevents 6-hyrodroxydopamine induced cytotoxicity and that it upregulates MANF expression and therefore employs MANF during its protective cascade. These findings therefore acknowledge MANF's significance as a neuroprotective agent and hence points to its future development as a potential agent against neurodegenerative disorders.

This work is wholeheartedly dedicated to my beloved parents, who have been my source of inspiration and gave me strength when I thought of giving up, who continually provide their moral, spiritual, emotional, and financial support.

ACKNOWLEDGEMENTS

First, I have to thank my research supervisor, Dr. Ram Mishra. Without his assistance in every step, this thesis would have never been accomplished. I would also like to thank my committee, including Dr. Bhagwati Gupta and Dr. Benicio Frey. Their insightful comments and encouragement incented me to widen my research from various perspectives. My time at McMaster University has been highly productive and working with Dr. Mishra was an extraordinary experience.

Getting through my dissertation required more than academic support, and I have many, many people to thank for listening to and, at times, having to tolerate me over the past three years. I cannot begin to express my gratitude and appreciation for their friendship. Judy, Ashley, Dima, Brendan, Sumitha, Vidhi and Brett have been unwavering in their personal and professional support during the time I spent at the University.

TABLE OF CONTENTS

LIST OF FIGURES

LIST OF TABLES

LIST OF ABBREVIATIONS

6-OHDA	6-hydroxydopamine
AKT	Protein kinase B
ANOVA	Analysis of variance
ATF	Activating transcription factor
CDNF	Cerebral dopamine neurotrophic factor
CHOP	C/EBP homologous proteins
CLC	Cardiotrophin-like cytokine
CNTF	Ciliary neurotrophic factor
CT-1	Cardiotrophin 1
DA	Dopamine
ER	Endoplasmic reticulum
GDNF	Growth-derived neurotrophic factor
GRP-78	Glucose-regulated protein 78
IL	Interleukin
IRE	Inositol-requiring enzyme
LIF	Leukemia inhibitory factor
MANF	Mesencephalic astrocyte-derived neurotrophic factor
MMP	Mitochondrial membrane potential
mTOR	Mammalian target of rapamycin
NGF	Nerve growth factor
NPN	Neuropoetin
NTF	Neurotrophic factor
OSM	Oncostatin M
PD	Parkinson's Disease
PERK	Pancreatic ER kinase-like kinase
PI3K	Phosphoinositide 3-kinase
PPAR	Peroxisome proliferator activated receptors
PPRE	Peroxisome proliferator response elements
ROS	Reactive oxygen species
SAPLIPS	Saposin-like proteins
shRNA	Short hairpin RNA
TGF	Transforming growth factor
UPR	Unfolded protein response
XBP1-s	spliced X-box binding protein 1

CHAPTER 1- Introduction

1.1 Parkinson's Disease

1.1.1 The Epidemiology Parkinson's Disease

Parkinson's disease (PD) is a chronic neurological disorder that progresses over time and is the second most common neurological disorder affecting an estimated 55,000 Canadians aged 18 and above (Wong, Gilmour, & Ramage-Morin, 2014). PD is characterized by a loss of dopaminergic (DA) neurons in the midbrain, specifically in the substantia nigra (SN)(Agid, 1991).

According to a review of conducted in 2016, PD's incidence rate is estimated to be approximately 17 per 100,000 people yearly (Hirsch, Jette, Frolkis, Steeves, & Pringsheim, 2016), which is therefore an indicator of a substantial societal and economic burden estimated to be $1.5 billion annually (Huse et al., 2005).

PD is less prevalent before the age of 50 years and its incidence increases with increasing age up to an age of 90 years(Wong et al., 2014). The prevalence of PD is higher in males than females and its incidence is estimated to triple over the next 50 years, which is attributed to the increase in life expectancy and of the average age of the population in the future (Wong et al., 2014).

1.1.2 The Pathophysiology of PD

Motor deficits within PD patients are mainly attributed to the lack of DA signaling due to the loss of more than 50% of DA nerve terminals within the striatum (Agid, 1991). The execution of motor functions occurs through a neural network that connects the cerebral cortex, the thalamus and the basal ganglia (Blandini, Nappi, Tassorelli, & Martignoni, 2000). The basal ganglia circuit is situated between the

thalamus and the cortex and its main role entails processing the neural signal flowing from the cortex thereby producing an output signal that eventually returns to the cortex, allowing for the execution of movement (Blandini et al., 2000). The ability to control voluntary movement within PD is lost as a consequence of severe perturbations to this pathway.

A DA pathway, known as the nigrostriatal pathway, connects the SN with the dorsal striatum and is involved in motor functions through the basal ganglia motor system (Agid, 1991) (Figure 1). The circuitry of the basal ganglia consists of five nuclei, including the globus pallidus, the caudate and putamen (collectively known as the striatum), the SN and subthalamic nucleus(Blandini et al., 2000). The loss of DA within the SN (specifically within the SN pars compacta (SNpc)) eventually affects the basal ganglia's ability to coordinate excitatory and inhibitory motor signals, leading to a decrease in motor output in what is known as hypokinesia (Agid, 1991). Common symptoms associated with PD include rigidity (increased muscle resistance to movement of a joint), bradykinesia (reduced voluntary movement), reduced balance, orientation and postural control, gait impairment and dyskinesia (physically tiring abnormal movements of the head, neck and limbs) (Agid, 1991).

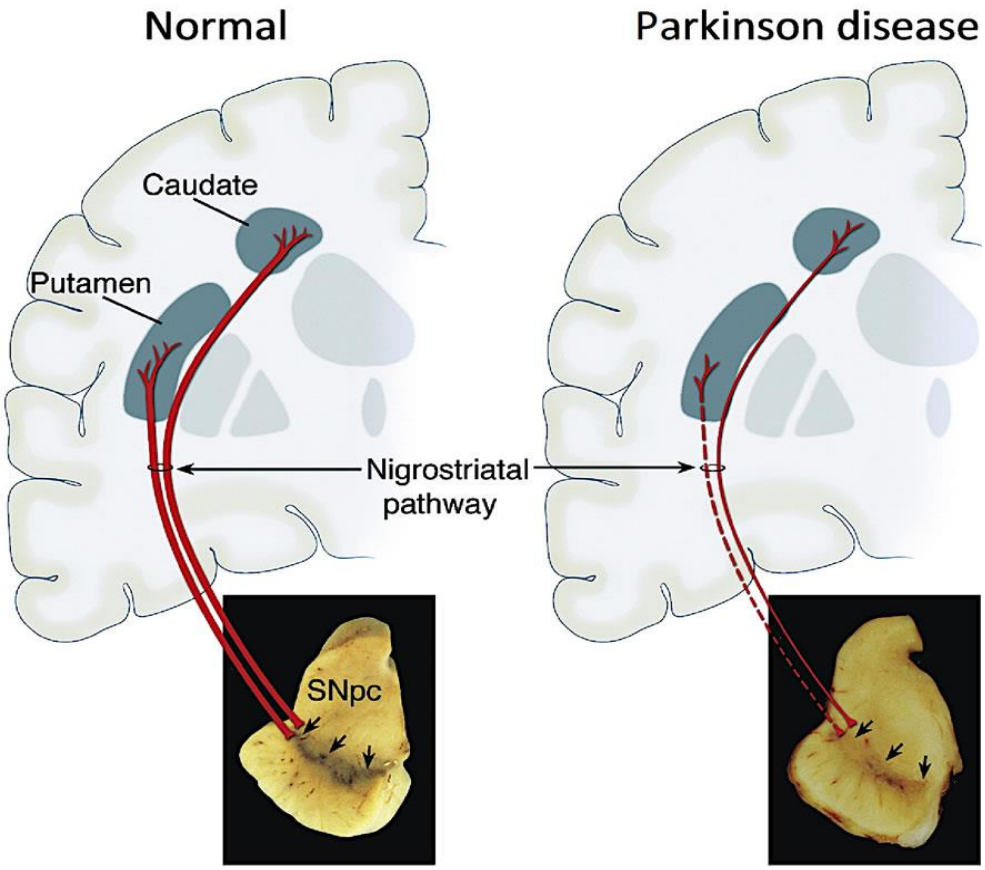

Figure 1: The characteristic DA neuron depletion in the SNpc of PD patients. The image on the left shows the intact nigrostriatal pathway signaling between the SNpc and the putamen and caudate nuclei (striatum) as well as the presence of staining within the SNpc due to neuromelanin containing DA neurons(Dauer & Przedborski, 2003). In the PD state, shown on the right, the absence of DA neurons (and hence the absence of the staining) leads to manifestation of motor deficits due to the perturbation to the nigrostriatal pathway signaling(Dauer & Przedborski, 2003).

1.1.3 PD and Oxidative Stress

PD is supposedly caused by the combined effects of genetic predispositions and environmental factors that lead to the death of DA neurons within the SNpc. The growing interest for genetic predispositions was due to the discovery of familial cases of PD. The apoptotic pathway is initiated through the increased levels of oxidative stress within DA cells, demonstrated by the ability of oxidizing toxins to induce neural degeneration(Blesa, Trigo-Damas, Quiroga-Varela, & Jackson-Lewis, 2015).

Free radical production and increased levels of reactive oxygen species (ROS), changes in catecholamine metabolism, mitochondrial dysfunction as a well as a lack of anti-oxidants have been identified as major contributors to the degeneration of DA neurons and the pathogenesis of PD (Jenner, 2003). Moreover, the increased vulnerability of DA neurons with aging is attributed to the progressive decline in levels of normal cellular processes such as antioxidant production that combat such stressors(Jenner, 2003).

ROS production occurs continuously throughout the body, however the imbalance between ROS production and levels of antioxidants leads to the elevation of oxidative stress and may eventually cell death (Blesa et al., 2015) (Figure 2). Dysfunctions in the ubiquitin-proteasome system (UPS) that target proteins for degradation, may also contribute to the aggregation of protein and oxidative stress(Blesa et al., 2015).

Studies have shown that the oxidative stress sensors, such as nuclear factor-kappa B, are increased within PD patients. The formation of Lewy bodies (abnormal aggregates of protein that develop inside nerve cells), composed of a protein called alpha-synuclein,

leads to the displacement of other cell components and is a contributor to oxidative stress (Jenner, 2003). Moreover, complex I dysfunctions in the electron transport chain within the mitochondria leads to the increase in lewy-body inclusions and is one of the major contributors to the elevation of ROS and the activation of apoptotic pathways downstream(Jenner, 2003).

Alpha-synuclein is a small unfolded protein that aggregates toxically within the cytoplasm due to mutations in the SCNA gene(Spillantini et al., 1997). The aggregation and subsequent apoptosis caused by alpha-synuclein leads to the decrease in DA signaling between the SN and the striatum within the basal ganglia, thereby increasing inhibitory signals to the thalamus and the motor cortex (Spillantini et al., 1997). This in turn causes the characteristic loss in motor coordination exhibited by PD patients.

Around 15% of PD cases are attributed to genetic factors and genome-wide association studies have revealed multiple genetic mutations to be risk factors contributing to familial PD(Shulman, De Jager, & Feany, 2011). The most common mutations include SNCA; LRRK2 coding for leucine-rich kinase 2 which affects the protein's kinase activity and is the most common cause of familial PD; PARK2 coding for parkin, which is a ubiquitin ligase that is involved in mitochondrial biosynthesis and can lead in disruption of the respiratory chain and subsequent oxidative stress leading to early onset of PD(Shulman et al., 2011).

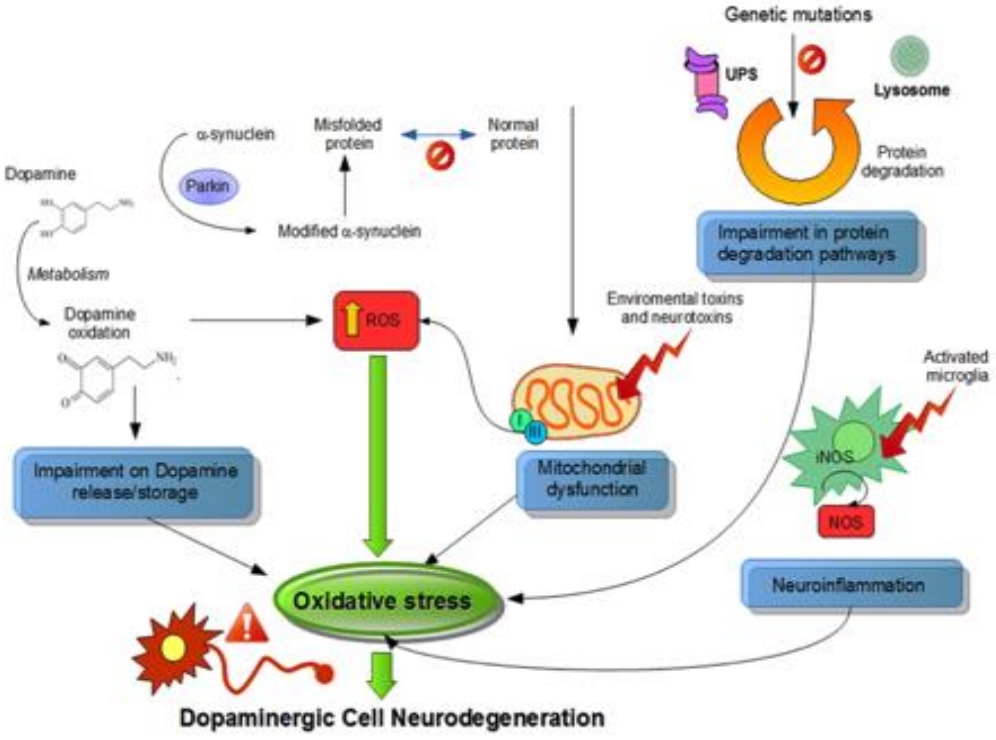

Figure 2: Schematic representation of the various mechanism that lead to oxidative stress. Factors such as mitochondrial dysfunction, DA auto-oxidation, neuroinflammation, alpha synuclein aggregation as well as impairments to UPS leads to the increase in ROS levels and oxidative stress, which underlies the pathophysiology of neurodegenerative disorders such as PD (Blesa et al., 2015).

1.2 Neurotrophic Factors

Many studies have identified roles that neurotrophic factors (NTF) play in maintaining growth, survival and differentiation of neurons and other cell types within the central and peripheral nervous systems.

There are three main families of NTFs; the neurotrophin family, the transforming growth factor beta (TGF) family and the neurotrophic cytokines(Merja H. Voutilainen, Arumäe, Airavaara, & Saarma, 2015). The neurotrophin family act through the activation of the transmembrane receptor tyrosine kinase and includes brain derived NTF, nerve growth factor (NGF), neurotrophin-3 (NT-3) and neurotrophin-4/5 (NT-4/5). The TGF family NTFs are most relevant to DA neurons(Merja H. Voutilainen et al., 2015). The most widely studied NTFs in PD within this family are the glial-cell line derived NTF (GDNF) and neurturin, (Kordower & Bjorklund, 2013). GDNF has so far shown the greatest potential due to its ability to attenuate the 6-hydroxydopamine induced cytotoxicity of DA cells(Kordower & Bjorklund, 2013). However, GDNF has failed to produce any significant clinical benefits in phase II clinical trials. GDNF was also shown to be unsuccessful in attenuating oxidative stress and apoptosis in alpha-synuclein models of PD(Kordower & Bjorklund, 2013). The neurotrophic cytokines family includes secretory proteins such as ciliary neurotrophic factor (CNTF), cardiotrophin-1 (CT-1), leukemia inhibitory factor (LIF), neuropoietin (NPN), oncostatin M (OSM), cardiotrophin-like cytokine (CLC), interleukin 6 (IL-6), IL-11 and IL-27. These neurons act through transmembrane receptors and are mainly pertinent to the growth and survival of motor neurons(Merja H. Voutilainen et al., 2015).

Within the context of PD, the focus on NTFs is due to the symptomatic nature of current therapies and their failure in halting or reversing disease progression (M. H. Voutilainen et al., 2009a). The current pharmacological intervention involves the administration of levodopa (DA precursor)(LeWitt, 2008). Unfortunately, the

administration of dopamine is ineffective due to its inability to cross the blood-brain barrier. After crossing the blood-brain barrier, levodopa is converted to dopamine by the enzyme DOPA decarboxylase. However, such an intervention presents multiple limitations due to levodopa's low bioavailability and short half-life (LeWitt, 2008). Hence, clinical manifestation is inevitable and debilitating at the current state of the disease. Such challenges warrant the consideration of novel therapeutics and therefore the shift towards NTFs is currently gaining precedence due to therapeutic capacity within these proteins.

1.2.1 Mesencephalic Astrocyte-derived Neurotrophic Factor

The recently discovered family of NTFs, including the mesencephalic astrocyte-derived neurotrophic factor (MANF) and the cerebral dopamine NTF (CDNF) , have proven to be interesting candidates to study within the context of PD because these NTFs are involved in endoplasmic reticulum (ER) homeostasis and the unfolded protein response (UPR), both of which are abnormal in PD (Lindahl, Saarma, & Lindholm, 2017). MANF and CDNF represent an evolutionary conserved NTF family, identified in both invertebrate and vertebrate species and are mainly localized within the ER. MANF and CDNF have demonstrated to be neuroprotective against midbrain DA neuron degeneration in vitro(Lindahl et al., 2017). MANF and CDNF are unique in that they acts mainly within the cell, as opposed to other NTFs that are exclusively secreted, have a short amino acids sequence and do not require extensive processing and are therefore readily available within the cell(Lindahl et al., 2017).

The primary sequence of MANF contains an N-terminal signal peptide that directs it to the ER. Human MANF has a 179-amino acid sequence, and the cleavage of 21 amino acids results in the formation of the mature form of 158 amino acids (Figure 3) (Petrova et al., 2003; Z. Zhang et al., 2018). At the C-terminus, the MANF protein contains an RTDL sequence (Lys-Asp-Glu-Leu) for ER retention (Figure 3). Receptors within the Golgi body recognize the sequence and direct MANF back to the ER and hence it's localization within the ER(Lindahl et al., 2017).

MANF contains an N-terminal saposin-like lipid binding domain and a C-terminal SAP domain. These two domains act as two independent modalities (as opposed being tightly packed) and are believed to function in various cellular processes and intracellular trafficking(H. Liu, Tang, & Gong, 2015).

The N-terminal saposin domain is homologous to saposin-like proteins (SAPLIPs), which act as lipid and membrane binding proteins and has a globular architecture made up of five alpha helices(H. Liu et al., 2015) (Figure 3). The saposin domain contains a positively charged residue on the outer surface that is believed to be involved in the membrane interaction. This domain is therefore believed to processes a similar structural and functional modality to the NK-lysin and granulysin SAPLIPs, that act against bacterial cells by targeting and disrupting the negatively charged lipid groups within their cell membranes(H. Liu et al., 2015).

The C-terminal SAP domain of MANF is made up of three alpha-helices and is structurally homologous to Ku70 proteins. Ku70 proteins function as antiapoptotic proteins in the cytoplasm by binding to the proapoptotic protein Bax through its SAP

domain and keeps Bax in its inactive form. In vitro studies have demonstrated that MANF exhibited cytoprotective effects as efficiently as Ku70 and prevented apoptosis of neuronal cells(H. Liu et al., 2015). Moreover, Ku70 heterodimerizes with Ku80 proteins and processes a critical function in DNA double-strand break repair, however these has not yet been investigated with MANF(H. Liu et al., 2015).

Furthermore, at the C-terminus MANF contains a CXXC (127 cytesine-lysine-glycine-cysteine 130) motif, which in forming disulfide bridges act as disulfide oxidoreductases(Lindahl et al., 2017). These are often induced during ER stress and assist in protein folding (specifically in the formation of intramolecular disulfide bridges), and hence are thought to exert protective effects in attenuating ER stress caused by protein misfolding/aggregation(Lindahl et al., 2017).

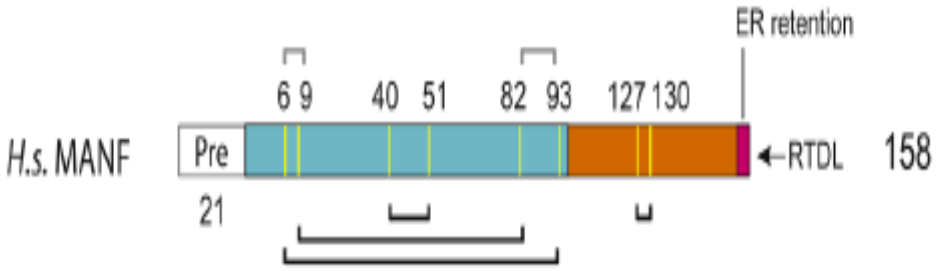

Figure 3: Schematic of the human MANF primary structure. The yellow lines represent the cysteine residues and the RTDL sequence for ER retention is represented at the C-terminus (Lindahl et al., 2017). The black bars underneath the sequence show the cysteine disulfide bridges. The blue region indicates the N-terminus saposin-like domain while the orange region represents the C-terminus SAP-like domain.

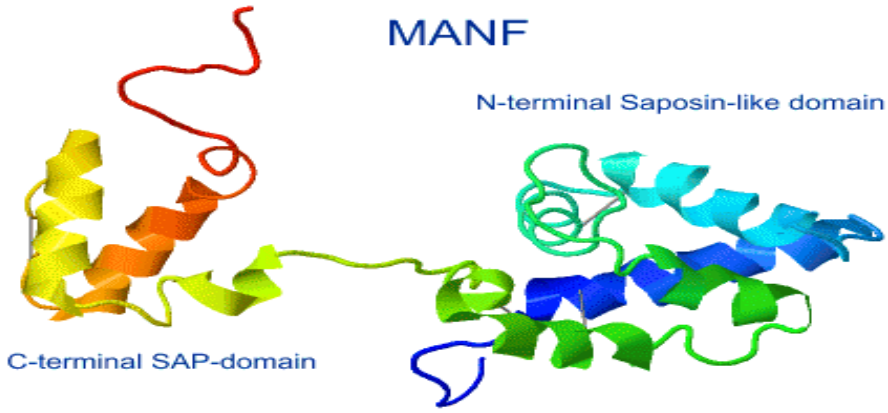

Figure 4: NMR structure of MANF. The blue-green region represents the N-terminus and the yellow-orange region represents the C-terminus. The N-terminus contains the saposin-like domain (amino acids 22-116) and the C-terminal domain contains the SAP domain (amino acids 117-179)(Danilova & Lindahl, 2018).

1.2.2 MANF and ER stress

ER stress can be caused by a number of factors including protein misfolding, protein aggregation, imbalance in protein production, reduction in ER calcium stores, errors in protein glycosylation and viral infections (Lindahl et al., 2017). The accumulation of such proteins in the ER lumen leads to ER stress and if prolonged causes apoptosis (Lindahl et al., 2017). Chronic ER stress is a major factor leading to the neurodegeneration of DA neurons and eventually resulting in PD (Lindahl et al., 2017). A defense mechanism, known as the UPR, alleviates ER stress by stopping protein translation, inducing the production of molecular chaperones that help in protein folding and degrading of misfolded proteins (Samali, FitzGerald, Deegan, & Gupta, 2010). The

UPR is mediated through three ER membrane receptors; pancreatic ER kinase-like ER kinase (PERK), activating transcription factor 6 (ATF6) and inositol-requiring enzyme 1 (IRE1) (Figure 5)(Lindahl et al., 2017). All three receptors are bound to an ER chaperone, known as glucose regulated protein 78 (GRP78), keeping them inactive (Figure 5A). The accumulation of misfolded proteins within the ER leads to the dissociation of GRP78 from PERK, ATF6 and IRE1 and thereby activating the UPR (Figure 5B) (Lindahl et al., 2017). MANF contains a promoter region for the ER stress response that is recognized by ER stress transcription factors, cleaved ATF6 and (spliced X-box binding protein) XBP1-s (Williams & Lipkin, 2006). Although MANF is mainly localized within the ER, during ER stress MANF secretion is increased (Lindahl et al., 2017). MANF was found to produce neuroprotective effects mainly by preventing ER stress, and thereby halting the apoptosis of DA neurons (Hao et al., 2017).

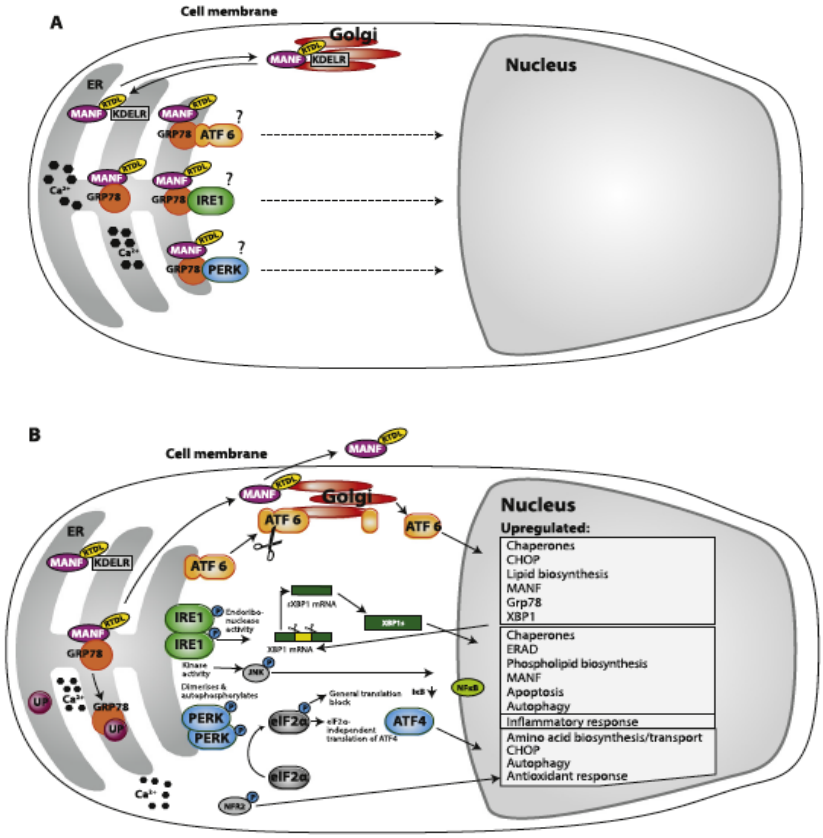

Figure 5: Representation of the UPR during ER stress and the role of MANF. (A) In the absence of ER stress, the UPR remains inactive through the binding of GRP78 to PERK, ATF6 and IRE1. MANF is localized within the ER via the RTDL sequence and is bound to GRP78 (which is interacting with UPR sensors) helping keep the UPR inactive. (B) During periods of ER stress, accumulation of misfolded proteins leads to the dissociation of GRP78 from PERK, ATF6 and IRE1 leading to the activation of the UPR. The lack of calcium stores leads to the dissociation of MANF from GRP78 and its increased secretion. IRE1 possesses an endoribonuclease activity, leading to the splicing of the X-box binding protein 1 (XBP1s) mRNA which acts as a transcription factor for various UPR elements. All the upregulated UPR factors by each of PERK, ATF6 and IRE1 are represented on the diagram (Lindahl et al., 2017).

1.3 Lentiviral-mediated shRNA knockdown

Lentiviral vectors are major tools used in research that allows for overexpression or silencing of genes, immunization against disease as well as generating transgenic models. Knockdown models by RNA interference or posttranscriptional gene silencing, uses short-hairpin RNA (shRNA) synthesized within the cell by a DNA construct that is delivered to the cell using a vector (Van den Haute, Eggermont, Nuttin, Debyser, & Baekelandt, 2003) (Figure 6). The use of a lentiviral vector for gene delivery has multiple advantages including the stable integration of the gene into the host genome allowing for long term expression as well as the delivery of large transgenic fragments.(Van den Haute et al., 2003).

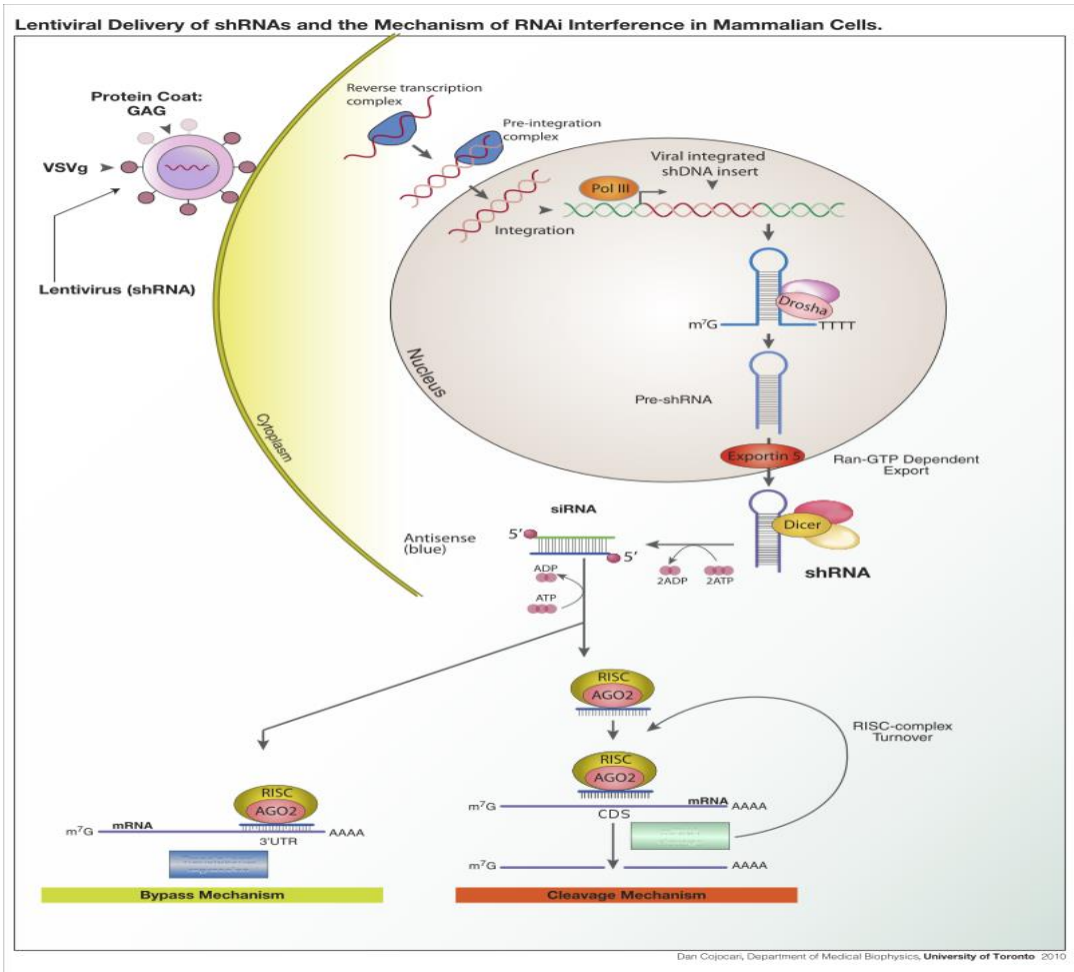

Figure 6: Schematic Representation of the mechanism of RNA interference using shRNA. The DNA construct enters the nucleus of the target cell. Double stranded RNA in the form of a shRNA is then continuously expressed from the construct (Van den Haute et al., 2003). The shRNA passes through the nuclear membrane into the cytoplasm of the cell, where an enzyme, Dicer, removes the loop converting the shRNA molecule into a short interfering RNA (siRNA) (Van den Haute et al., 2003). An enzymatic complex known as RISC, separates the siRNA into single strands (Van den Haute et al., 2003). One of the strands, the guide

strand, remains with the complex and binds to the target mRNA, cleaving it at a particular site. Therefore, the mRNA degrades and is silenced. Lentiviral-mediated shRNA delivery, is one of the most common, convenient and efficient ways in delivering shRNA into cells due to its low toxicity and its ability to deliver a large volume of viral RNA (Van den Haute et al., 2003). (By Dan Cojocari)

1.4 Curcumin and its Therapeutic Role

The phytochemical curcumin is a bright yellow spice found in turmeric that has been traditionally used in India and in Asia for centuries as a treatment for a multitude of disorders including gastroenteritis, inflammation, cough, wounds, infections etc (J. Wang, Du, Jiang, & Xie, 2009). Curcumin is a polyphenolic flavonoid (1,7-bis[4-hydroxy 3-methoxy phenyl]-1,6-heptadiene-3,5-dione) (Figure 7) (J. Wang et al., 2009).

More recently, literature has elucidated curcumin's role and acknowledged its therapeutic potential due to its anti-oxidant, anti-cancerous, anti-viral, anti-bacterial, anti-fungal and iron-chelating activity (J. Wang et al., 2009). For example, curcumin was shown to be an attenuator of the incidence of colorectal cancer and it was shown to prevent the formation and buildup of plaques within arteries (Santel et al., 2008). Curcumin's anti-oxidant properties are modulated through its multiple molecular targets, including cytokines, enzymes and transcription factors. Curcumin's underlying mechanisms are believed to be extremely diverse and are continually being investigated (SHISHODIA, 2005; Tomita, Holman, Santoro, & Santoro, 2005).

Curcumin's role within neurodegenerative disorders such as PD and Alzheimer's disease has been studies extensively due to its ability to be administered at high dosages while demonstrating a very low toxicity(Mythri & Bharath, 2012). Studies have shown that curcumin could be administered daily at a dosage of around 12 grams per day with no reported toxicity(Dhillon et al., 2008). Moreover, the potential that curcumin withholds as a therapeutic for neurodegenerative disease lies within its ability to cross the blood brain barrier. The failure of curcumin to develop past clinical trials is due to its low bioavailability. Approximately 75% of curcumin fails to be absorbed across the intestinal mucosal barrier and is excreted in feces(Aggarwal & Harikumar, 2009). Furthermore, the portion of curcumin that is absorbed is metabolized by the liver and it is therefore rapidly eliminated. It has been concluded that such challenges reduce curcumins bioavailability to just around 1%, which would severely impact its ability to produce any cytoprotective effects(Aggarwal & Harikumar, 2009).

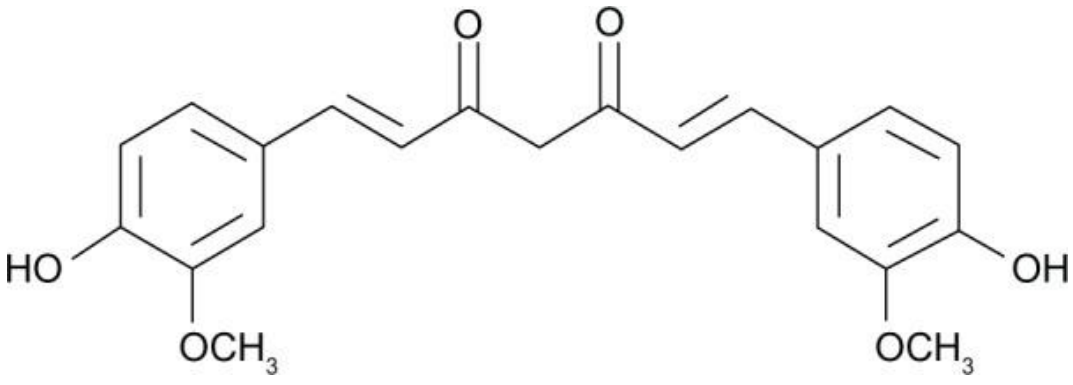

Figure 7: Structure of the polyphenolic flavonoid curcumin (1,7-bis[4-hydroxy 3-methoxy phenyl]-1,6-heptadiene-3,5-dione)

1.5 6-Hydroxydopamine in vitro model of PD

6-hydroxydopamine (6-OHDA) is a neurotoxin that is widely used in animal models of PD to selectively destroy DA neurons (Figure 8) (Deumens, Blokland, & Prickaerts, 2002). 6-OHDA's prevalent use is attributed to its ability to mimic the nigrostrial pathway degeneration and elevation of oxidative stress seen within PD patients (Deumens et al., 2002).

6-OHDA is a hydroxylated analogue of DA. Its preferential uptake by DA neurons allows for its accumulation within the cytoplasm and its induction of oxidative stress. One mechanism through which 6-OHDA acts was demonstrated through a reduction in antioxidant levels such as glutathione and superoxide dismutase following 6-OHDA administration(S.-F. Wang et al., 2017). The ROS formed by 6-OHDA leads respiratory inhibition and is specifically toxic to mitochondrial complex I leading to respiratory arrest(S.-F. Wang et al., 2017) (Figure 9). 6-OHDA can also lead to calcium dys-homeostasis, and leads to the activation of the calcium dependent cysteine-protease, calpain, which mediates the apoptotic pathway downstream. Moreover, 6-OHDA exhibits auto-oxidation and can independently take part in ROS forming reactions(S.-F. Wang et al., 2017).

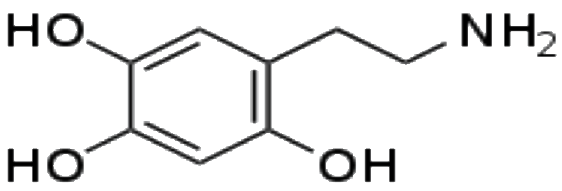

Figure 8: Structure of the neurotoxic agent 6-hydroxydopamine

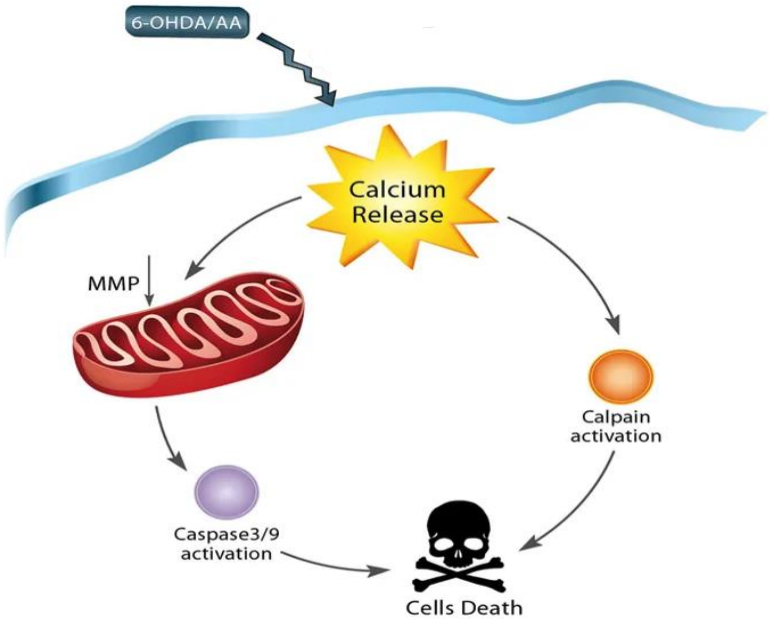

Figure 9: Mechanism of 6-OHDA-induced cytotoxicity. 6-OHDA acts by increasing the levels of ROS and reducing the levels of anti-oxidants in the cell. 6-OHDA induced calcium dysregulation leads to the activation of calpain proteins. Moreover, disruption of the mitochondrial membrane potential (MMP) leads to the activation of caspase proteins (a class of protease that mediate the apoptotic pathway)(S.-F. Wang et al., 2017).

1.6 The mTOR pathway

The mammalian target of rapamycin (mTOR) pathway is the master regulator of cell survival, growth and proliferation. Multiple studies have clearly outlined the importance of the pathway in regulating cell processes such as apoptosis, metabolism and ribosomal biogenesis through integrating multiple signals from growth, energy and

nutrient factors(Laplante & Sabatini, 2009). Hence, it has been clearly associated with the pathophysiology of various disease such as cancer and diabetes.

The mTOR protein is a 289 kDA serine-threonine kinase and is evolutionary conserved(Laplante & Sabatini, 2009). The two mTOR proteins are mTOR complex 1 (mTORC1) and mTOR complex 2 (mTORC2). mTORC1 is the master regulator cell growth and metabolism and is a positive regulator of cell survival by activating and promoting anabolic processes including lipid and protein biogenesis and by negatively regulating apoptosis (Laplante & Sabatini, 2009)(Figure 35).

mTORC1 is stimulated by growth factors such as insulin (Figure 34). For example, the binding of insulin enhances the tyrosine kinase activity of insulin's cell surface receptor. This in turn leads to the activation of phosphoinositide 3-kinase (PI3K), which then phosphorylates protein kinase B (AKT), which then finally leads to the activation of mTOR downstream(Laplante & Sabatini, 2009).

The knowledge about mTORC1 came about through the use of the bacterial macrolide (a class of antibiotics) rapamycin. Rapamycin is an inhibitor of mTORC1 and we can therefore utilize it to investigate the involvement of the mTOR pathway within the function of curcumin and its effects on its therapeutic functions(Laplante & Sabatini, 2009).

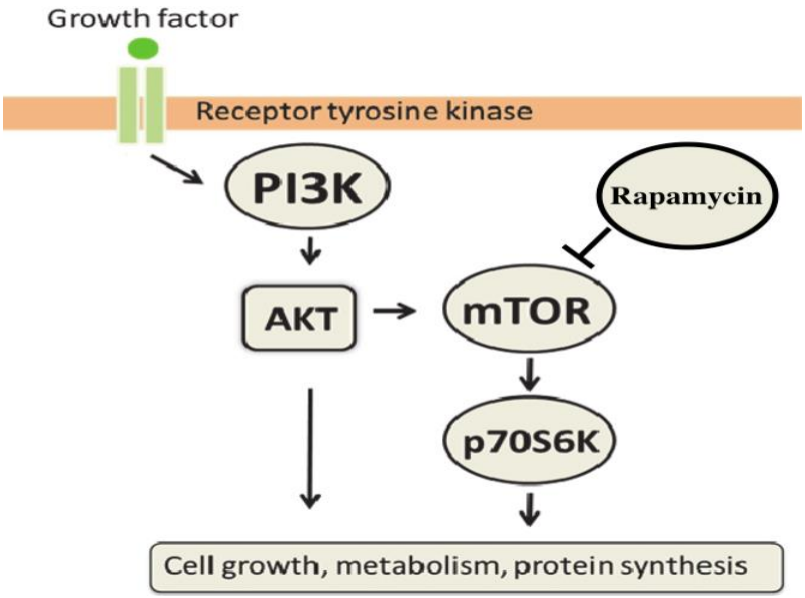

Figure 10: Mechanism of mTOR activation. In the example here, the PI3K is activated by receptor tyrosine kinase. PI3K then leads to AKT phosphorylation and subsequent mTOR activation. Rapmycin is shown as an mTOR blocker**.**

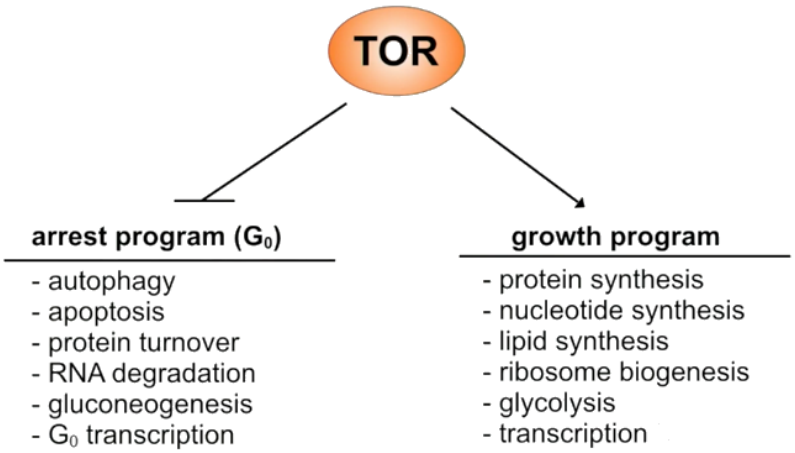

Figure 11: List of mechanisms that are activated and deactivated by the mTOR pathway.

1.7 Study Rationale

1.7.1 Lentiviral-shRNA knockdown of MANF in vivo

In vitro models have been successful in identifying and representing the potential that MANF withholds as a future therapeutic against DA neuron degenerations, but have failed to identify the mechanism of action of MANF as well as its significance as a model of PD or its ability in attenuating clinical manifestations and disease progression(M. H. Voutilainen et al., 2009).

Moreover, the most widely used neurotoxic agents that model PD in rodents, including 6-OHDA and MPTP, mimic DA neuron degeneration, but hold characteristics that differ drastically from clinical manifestations and the pathophysiology of PD(Blesa & Przedborski, 2014). These differences include the accelerated degeneration of DA neurons in rodents compared to humans, exclusively dopaminergic lesions and inconsistencies in the observed behavioral and motor deficits(Blesa & Przedborski, 2014). The lack of an in vivo model to characterize key pathophysiological features of PD presents us with a significant barrier to our understanding of the disease and how to treat it.

We are proposing a rodent knockdown model of MANF that will provide great insights into the role of MANF, its mechanism of action and its ability to halt or reverse disease progression and thereby paving the way for its clinical development as a therapeutic.

1.7.2 Curcumin's neuroprotective properties against 6-OHDA induced cytotoxicity

Curcumin's neuroprotective properties have been widely explored, however, its mechanism of action remains an enigma that continues to be explored. We aim to assess curcumin's neuroprotective properties in vivo and quantify its ability to attenuate ER stress induced cytotoxicity. 6-OHDA as a toxin would allow for recapitulation of neuronal diseases associated with DA neuron depletion and for modelling the hypothesized effects of curcumin on MANF and its downstream effects on cell survival. The link between curcumin and MANF's expression would therefore be elucidated in the context of an established model of PD's pathophysiology and allows for the investigation of their underlying mechanisms. Moreover, we aim to explore whether the mTOR pathway is involved within curcumin's mechanism of action, through utilization of the mTOR pathway blocker rapamycin.

The aims of this project serve to generate a potential model of PD that presents a rigorous recapitulation of both clinical and pathophysiological perturbations. Moreover, this model will give us insight into the role of MANF, its mechanism of action and its therapeutic potential within the context of ER stress, DA neuron degeneration and PD.

CHAPTER 2- Investigating the effect of MANF knockdown on ER stress and the pathophysiology of PD

2.1 Aims

We aim to establish a knockdown model of MANF and investigate the pathophysiology of PD both behaviourally and molecularly;

1. Investigation of MANF's role in ER stress using an in vivo MANF knockdown model of PD. Administration of the knockdown will occur through using short hairpin RNA (shRNA) that is used to cleave mRNA target and therefore allows for post-transcriptional gene silencing. The shRNA will be delivered using a lentiviral vector.
2. Assessing whether MANF knockdown rats retain behavioural and motor deficits of PD compared to controls. The performance on a variety of the most commonly used motor functions tasks will be performed, mainly the beam-transversal test (assesses the dysfunctions in motor coordination that is brought by PD), cylinder test (assesses forelimb assymetry) and the rotarod test (tests forelimb and hindlimb coordination) consistently over a ten-month period. Following behavioural analysis we will be able to gain an understanding of the importance of MANF within disease progression and specifically its ability to model motor perturbations that are characteristic of PD.
3. Investigation of the pathophysiology of the MANF knockdown model by quantifying the degree of DA neuron depletion and ER stress that has resulted from the absence of MANF through analyzing mRNA expression levels of

MANF (to confirm that the knockdown has occurred), ER stress markers and apoptotic markers.

2.2 Materials and Methods

2.2.1 Animals

12 Male Sprague Dawley rats at a weight of 250-300 grams were obtained from Charles River, Canada. Upon arrival, rats were housed individually in cages at the central animal facility at McMaster University and were given one week to acclimatize to the environment. All methods and procedures were approved by the central animal facility while complying to the Guide to Care and Use of Experimental Animals. Rats were exposed to constant 12-hour light/dark cycles at a temperature of 22º Celcius and 50% humidity. The rats were given *ad libitum* access to water but were food restricted to 90% of their free-feeding body weight.

2.2.2 Lentiviral shRNA Knockdown

The rats were divided into two groups, n=6 for the MANF knockdown group (Lentiviral vector mediated shRNA knockdown of MANF in the SN) (shMANF) and n=6 control (scrambled control was administered using the lentiviral shRNA to this group) (shCtrl).

Stereotaxic surgery was utilized to administer the lentiviral vector. The SN was first located in reference to bregma (Anterior/Posterior=-5.3 mm, Medial/Lateral=±2.3 mm, Dorsal/Ventral=-7.8 mm). The lentiviral vector was then administered unilaterally into the SN using the UMP3 UltraMicroPump (World Precision Intruments, Inc).

2.2.3 Behavioural Analysis

Behavioural analysis was conducted consistently over a ten-month period and included the following tests;

Beam Transversal Test: This test consists of a 1 meter beam that is 1.5 cm wide. The beam is placed between two raised platforms (Figure 10). The rat is placed on one side and is made to cross the beam to reach an enclosed chamber, where a fruit loop is given as a reward. The test is repeated 3 times to yield an average result of all the parameters. The rats were first trained over a period of three weeks on the beam before any testing took place. The test measures latency time to traverse, transversal time as well as ipsilateral and contralateral hind limb slips. The test will assess balance and sensorimotor coordination which are effective and reliable measures used to assess the basal ganglia dysfunction that is brought by PD including the detection of the perturbations of the nigrostriatal pathway(Brooks & Dunnett, 2009).

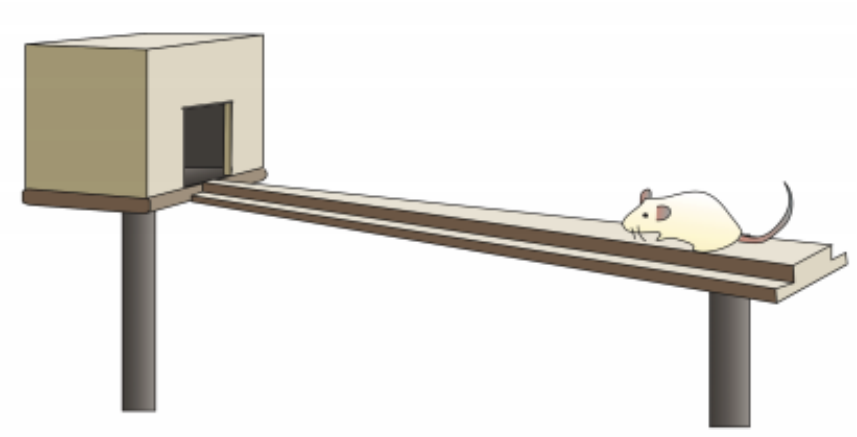

Figure 12: The narrow beam transversal test (Brooks & Dunnett, 2009).

1. R**otarod test:** This is a fixed speed motor driven rod (Digital Rota Rod, Bluefic Rotarod, India) that tests motor functions, specifically forelimb and hindlimb coordination and is and effective test for analyzing motor deficits in rodent(Brooks & Dunnett, 2009). The rats were placed on the opposite direction of the rotating rod and the goal is to maintain balance (Figure 11). A switch is present underneath the rod and is used for recording the time taken until the rat falls. The speeds used are 10 and 20 RPM and each rat performed the test 3 times at each speed and then an average of the trials is used.

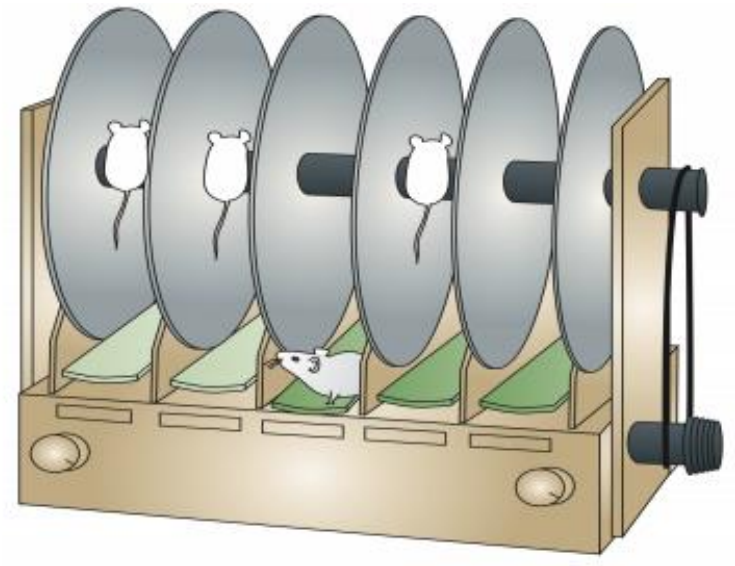

Figure 13: The fixed speed-rotating rod (Brooks & Dunnett, 2009).

Cylinder test: This test assesses locomotor asymmetry that is brought by unilateral deficits in lesion studies. Through utilization of the rat's exploratory behaviour and the percentage of forelimb ipsilateral (i.e. the side of the body that is opposite of the shRNA knockdown) touches, the test assesses the asymmetry present in favoring one forelimb over the other(Brooks & Dunnett, 2009). The test is performed by placing the rat in the unfamiliar cylinder environment and recording the total of 20 forelimb touches and the score is expressed as the number of ipsilateral touches per 20 touches (Figure 12).

Figure 14: The cylinder test chamber.

2.2.4 Sacrifices

Rats were sacrificed by using isofluorane (Pharmaceutical Partners of Canada Inc, Richmond hill, Ontario, Canada) as an anesthetic and decapitation. The brain was then de-skulled and sectioned. The brain samples collected for analysis were the SN, striatum and cortex. The tissue samples were first flash frozen in dry ice and then stored at -80^{o} Celcius.

2.2.5 RNA extraction

Total RNA was extracted via manufacturer's instructions using TRIzol reagent (ThermoFisher Scientific, Catalog#15596018). Tissues were first homogenized in 1ml of the TrIzol reagent. Following complete dissolution of the brain tissues, the solution was incubated at room temperature for five minutes. 0.2ml of chloroform was then added to the solution, and it was shaken for 15 seconds. The solution was then centrifuged at 12000g for 15 minutes at 4^{o} Celcius. The colorless RNA phase was then transferred to a 1.5ml eppendorf tube and to the tube 0.5 ml of isopropanol was added. The solution was then shaken for 15 seconds and centrifuged at 12000g for 10 minutes at 4^{o} Celcius. The supernatant was removed and then 1ml of 75% ethanol was added to the RNA pellet. The solution was again centrifuged at 7500g for 5 minutes at at 4^{o} Celcius. The ethanol was removed and the pellet was allowed to air dry for 10 minutes. The pellet was dissolved in 40uL od DEPC-treated water and heated in a water bath at 60^{o} Celcius for 10 minutes. RNA concentration and purity were determined using the NanoDrop 2000 Spectrophotometer measuring absorption at 260nm and 280nm. Genomic DNA was removed using the DNAse I enzyme (ThermoFisher Scientific, Catalog#EN0521).

2.2.6 cDNA synthesis

Complementary cDNA was made by reverse transcription using the qScript cDNA SuperMix (QuantaBio, Catalog#95048-100). To determine Real Time-quantitative PCR (RT-qPCR) specificity and to check for any contamination, negative reverse transcription controls were made for random samples without the addition of the reverse transcriptase enzyme.

2.2.7 Real-Time Quantitative Reverse Transcription PCR (RT-qPCR)

Rat MANF, GRP78, the transcription factor C/EBP homologous protein CHOP and the housekeeping gene GAPDH primers were used for qPCR analysis (Table 1). All primers were synthesized at the MOBIX lab facility (McMaster University, Canada) and primer identity was verified by running the PCR product of a test sample on 1.5% agarose gel. The agarose bands were then excised and sent to the MOBIX (McMaster University, Canada) lab for sequencing.

The final concentration of all primers used was 1μM. RT-qPCRs were carried out as per manufacturer's specifications of SYBR Green PCR kit (Qiagen CAT # 204056) using 96-well plates. Conditions used were 95°C for an initial 5 minutes followed by 40 cycles of denaturation at 95°C for 10 seconds and annealing at 60°C for 30 seconds. No template control of nuclease free water was used for every plate. The specificity of the amplified product was determined by the melting curve analysis producing a single peak.

Each reaction 25 uL containing 60ng of total RNA (2ul of cDNA and 23 uL of a master mix containing 12.5ul of SYBR Green, 5ul of forward and 5ul of reverse primers and 0.5ul of nuclease free water).

Each sample was analyzed in triplicates and Ct values were limited to a variability of ±0.5 using the Stratagene MX3000P cycler (Figure 13; Figure 14; Figure 15). Arbitrary mRNA concentrations were calculated by the Bio-Rad software, using the relative standard curve method. Relative gene expression was compared using the delta-delta Ct method of analysis, were average Ct values for MANF, GRP78 and CHOP were normalized to GAPDH Ct values and the following equation was used:

$\Delta\Delta Ct = 2^{-\Delta\Delta Ct}$

$\Delta\Delta Ct$= ((Ct-Gene of interest–Ct-Housekeeping)–(Ct-Avg Ctrl Gene of interest–Ct-Avg Ctrl Housekeeping).

Genes	**qPCR primers (5'→3')**
MANF	**Forward:** CGGTTGTGCTACTACATTGGA; **Reverse:** CTGGCTGTCTTCCTTCTTGACC
GRP78	**Forward:** CTGGGTACATTTGATCTGACTGG; **Reverse:** GCATCCTGGTGGCTTTCCAGCCATTC
CHOP	**Forward:** GTCTCTGCCTTTCGCCTTTG; **Reverse:** CTACCCTCAGTCCCCTCCTC
GAPDH	**Forward:** CAACTCCCTCAAGATTGTCAGCAA; **Reverse:** GGCATGGACTGTGGTCATGA

Table 1: Rat RT-qPCR forward and reverse primer sequences.

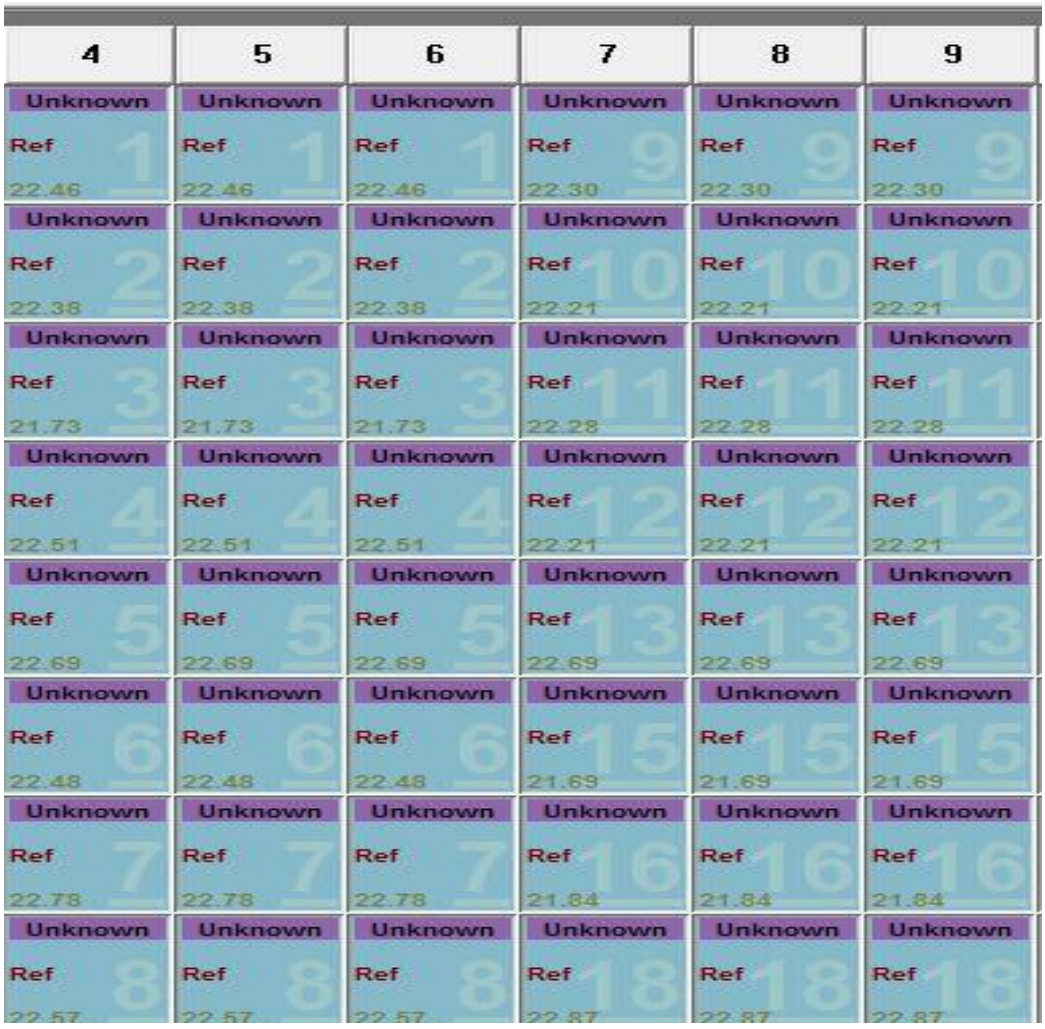

Figure 15: RT-qPCR output of the MX300P software. Samples were run in triplicates. The Ct values are represented for each well. The Ct values all fall within a range of ±0.5 of the median value.

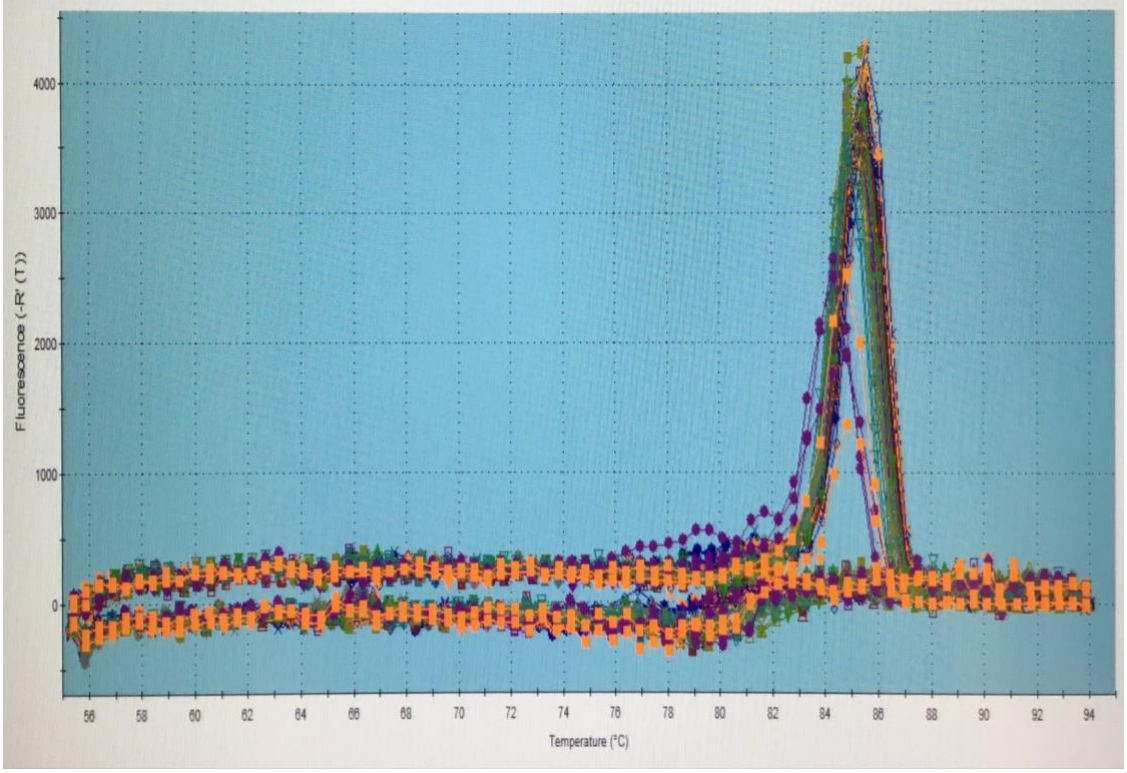

Figure 16: RT-qPCR Dissociation curve. Samples were run in triplicates. The plot shows one peak, which represents the amplification of one gene product. The X-axis represents the temperature and the Y-axis represents the fluorescence.

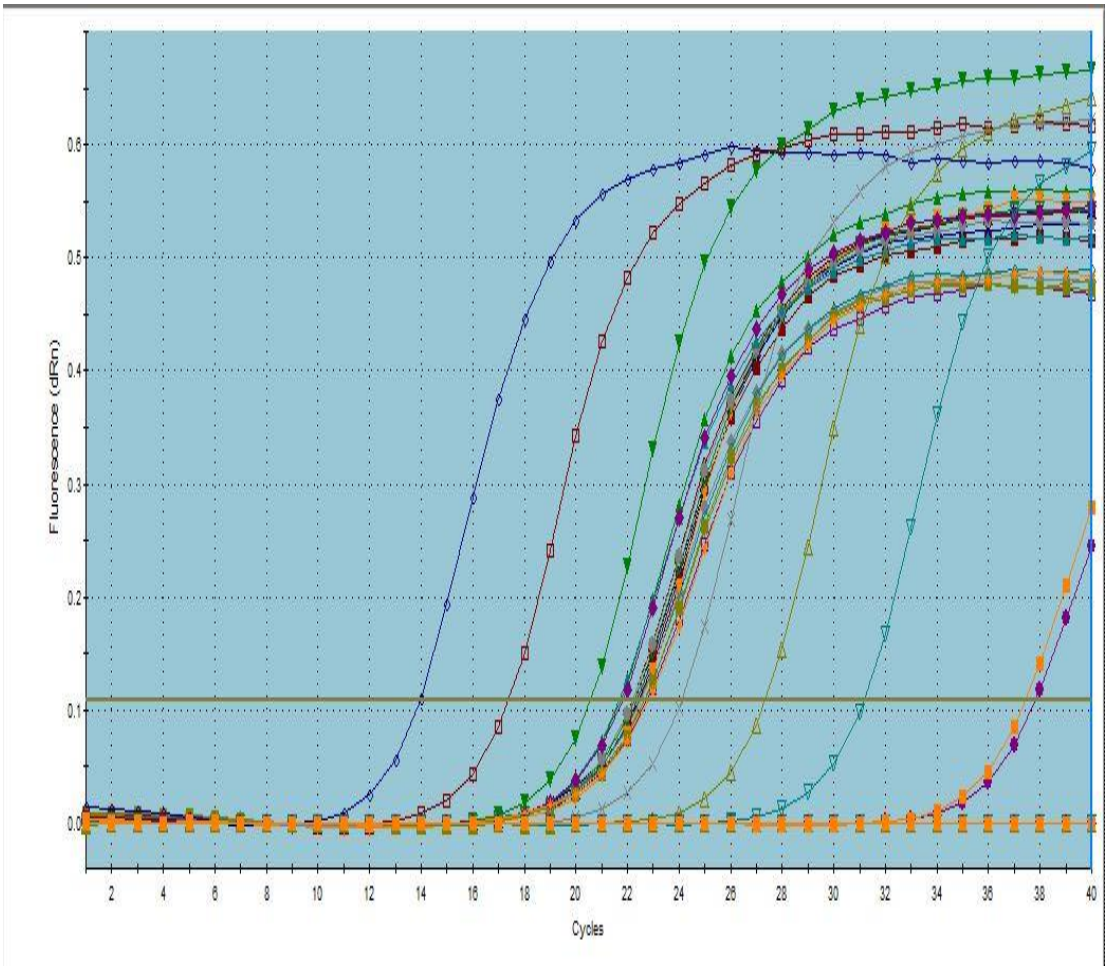

Figure 17: RT-qPCR Amplification plot. Each color represents one sample. The X-axis represents the cycle number and the Y-axis represents the fluorescence.

2.2.8 Statistics

All statistical analyses were carried out using GraphPad Prism 6.0 software (GraphPad Software, USA). Before analyses, outlier detection was performed using the GraphPad Outlier Tool. One-way analysis of variance (ANOVA) with Tukey's post-hoc was used as a statistical test to determine difference between multiple groups and results containing only two groups were analyzed using an unpaired Student's t-test. For analysis of the beam transversal test, subject matching and two-way ANOVA was used. The relative standard curve method and the mRNA copy numbers were used to confirm no differences in the levels of the housekeeping gene GAPDH. In all statistical tests, significance was defined as $*p<0.05$, $**p<0.01$ and $***p<0.001$. Results are presented as plus or minus the standard error of the mean (SEM).

2.3 Results

2.3.1 The effect of Lentiviral-mediated shRNA knockdown of MANF on latency to fall

The fixed speed rotarod test was performed at two different speeds (10rpm and 20rpm to examine the latency time to fall and assess the forelimb and hindlimb motor coordination following MANF knockdown. The test revealed that at 10 rpm the shMANF group had a significantly shorter latency to fall ($p<0.05$), however, no significant differences were seen at 20rpm

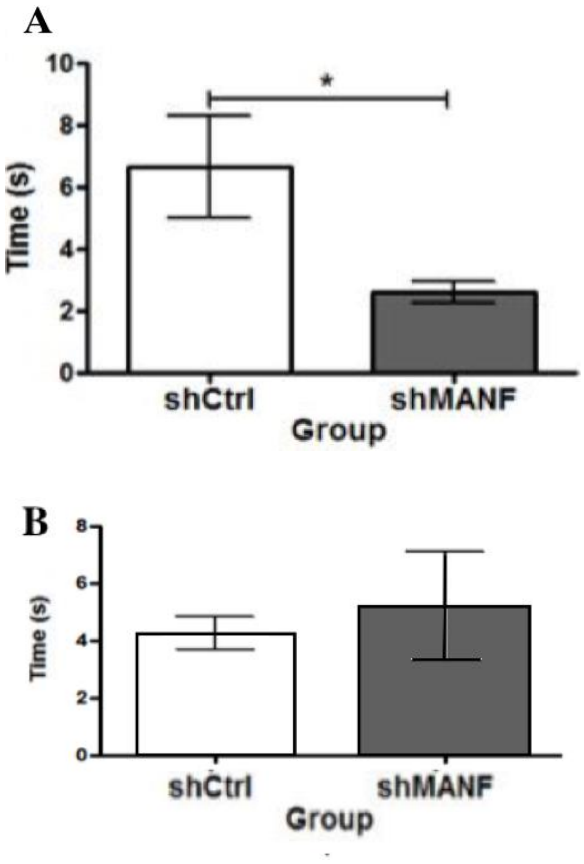

Figure 18: The rotarod test was performed three times at each speed and the mean time (in seconds) to fall was recorded. An unpaired t-test showed that at A) 10rpm the shMANF

group had a statistically significant shorter latency to fall ($p<0.05$) compared to the shCntrl and at B) 20rpm failed to show any statistically significant difference between the two groups ($p>0.05$)

2.3.2 The effect of Lentiviral-mediated shRNA knockdown of MANF on performance in the Beam Transversal Test

The rat's performance on the beam walk was consistently analyzed over a ten-month period following the knockdown to asses both the latency time to transverse and the transversal time. Two-way ANOVA showed that the shMANF group exhibited both significantly longer time to initiate movement (ANOVA $p<0.01$; Bonferroni test $p<0.05$) and a longer transversal time (ANOVA $p<0.01$; Bonferroni test $p<0.05$), which were strong indicators of the behavioural deficits that were incurred following the knockdown.

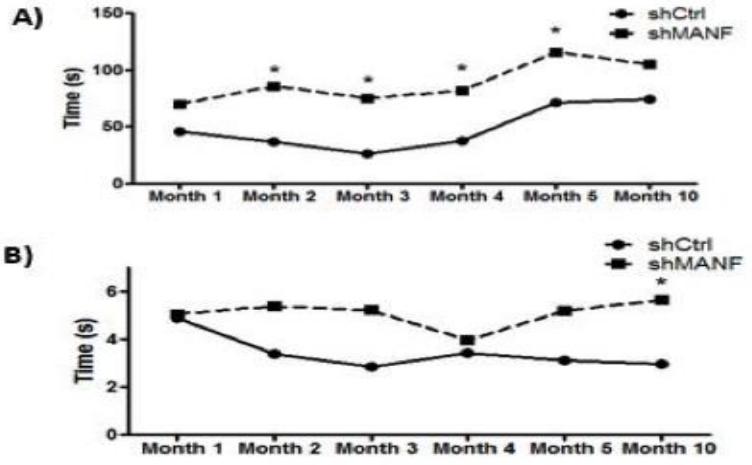

Figure 19: Performance on the beam transversal test was recorded as the mean time (in seconds) of three trials. (**A)** The latency time to transverse over the 10-month behavioral testing period. Two-way ANOVA revealed that the shMANF rats took a statistically

significant longer latency to transverse (ANOVA $p<0.01$; Bonferroni test $p<0.05$). (**4B)** The beam transversal time over the 10-month behavioral testing period. Results show that the shMANF group took a statistically significant longer transversal time (time to cross the beam) (ANOVA $p<0.01$; Bonferroni test $p<0.05$).

2.3.3 The effect of Lentiviral-mediated shRNA knockdown of MANF on forelimb asymmetry

Locomotor asymmetry was assessed using the cylinder test to reveal whether the MANF knockdown rats favoured the ipsilateral limb as a result of the knockdown. The test introduces the rats to an unfamiliar environment and the limb with which the touch is performed was recorded over 20 trials. The results revealed that the shMANF group significantly favoured the ipsilateral side ($p<0.01$).

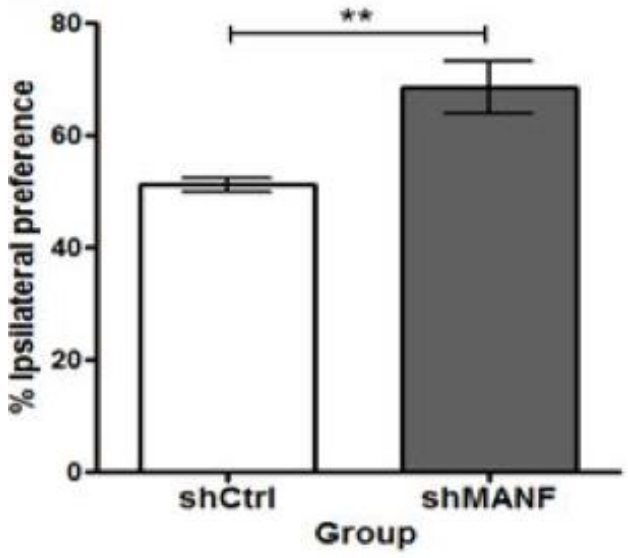

Figure 20: The cylinder test was performed to assess locomotor asymmetry following MANF knockdown. The test was scored by recording the number of

ipsilateral forelimb touches per 20 total touches. The test showed a statistically significant increase in the percent of ipsilateral touches in the shMANF group ($p<0.01$).

2.3.4 The effect of Lentiviral-mediated shRNA knockdown of MANF on MANF mRNA levels in the SN

Following 10 months of behavioural testing, rats were sacrificed, and cDNA was prepared. RT-qPCR analysis of MANF mRNA in the SN was performed to confirm that the knockdown was successful. The shMANF group had a significantly lower expression of MANF ($p<0.05$).

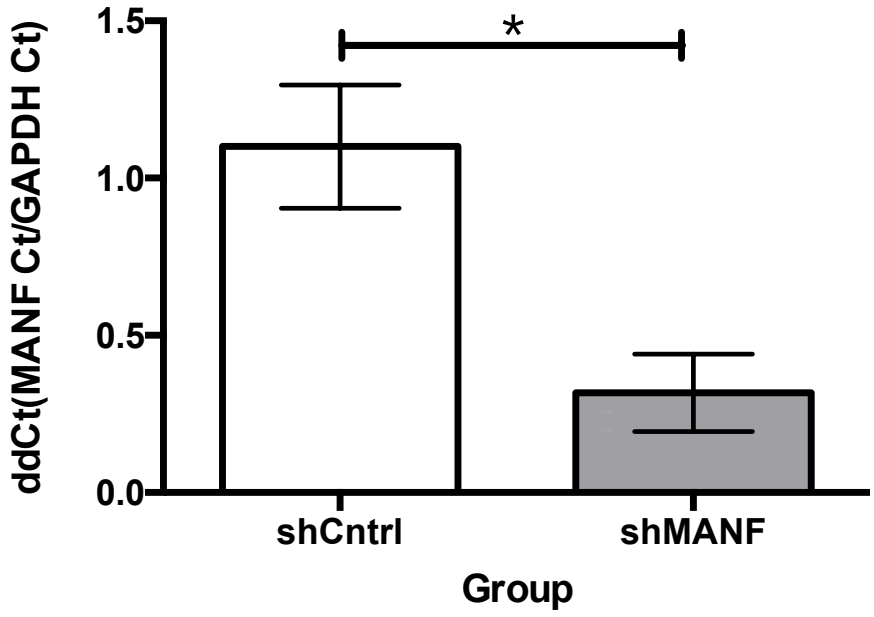

Figure 21: RT-qPCR analysis using the delta-delta Ct method and the unpaired t-test showed a statistically significantly reduced expression of MANF mRNA following lentiviral-mediated shRNA knockdown ($p<0.05$)

2.3.5 The effect of Lentiviral-mediated shRNA knockdown of MANF on the mRNA levels of the ER stress marker GRP78 in the SN

The mRNA level of the ER stress marker GRP78 in the SN was analyzed using RT-qPCR to analyze the effects of the knockdown on the chaperone's expression level. The shMANF group demonstrated a significantly reduced expression of GRP78 ($p<0.001$)

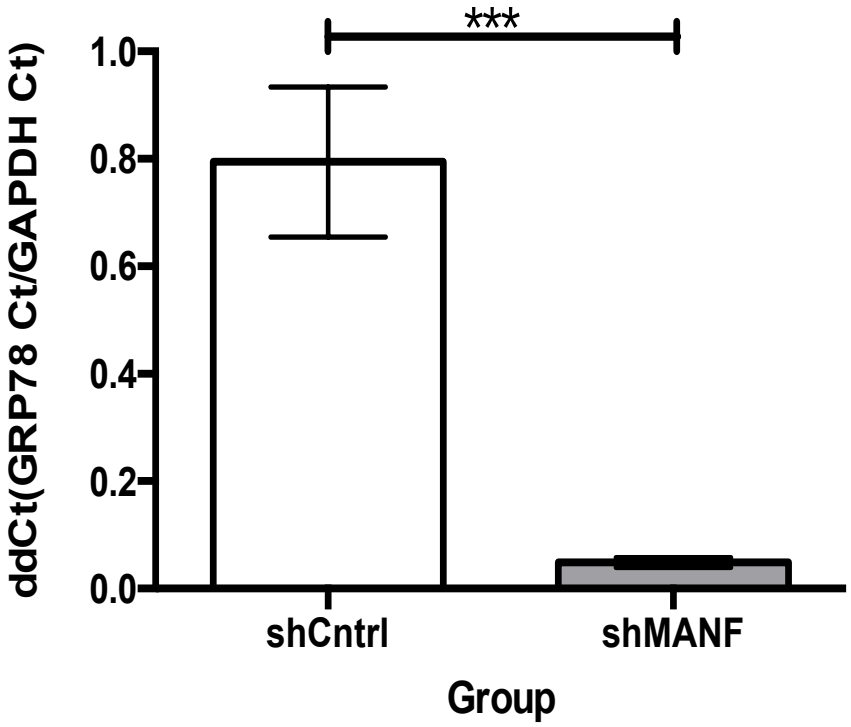

Figure 22: RT-qPCR analysis using the delta-delta Ct method and the unpaired t-test of the ER stress marker GRP78 showed a statistically significant reduced expression of GRP78 mRNA following lentiviral-mediated shRNA knockdown of MANF in the SN ($p<0.001$)

2.3.6 The effect of Lentiviral-mediated shRNA knockdown of MANF on the mRNA levels of the apoptotic marker CHOP in the SN

mRNA expression level of the apoptotic marker was assessed using RT-qPCR to analyze whether the knockdown of MANF led to the favouring of the apoptotic pathway in the SN. CHOP mRNA analysis is a strong indicator the level of DA neuron depletion in the SN. The expression level of CHOP was statistically increased as a result of the knockdown ($p<0.05$).

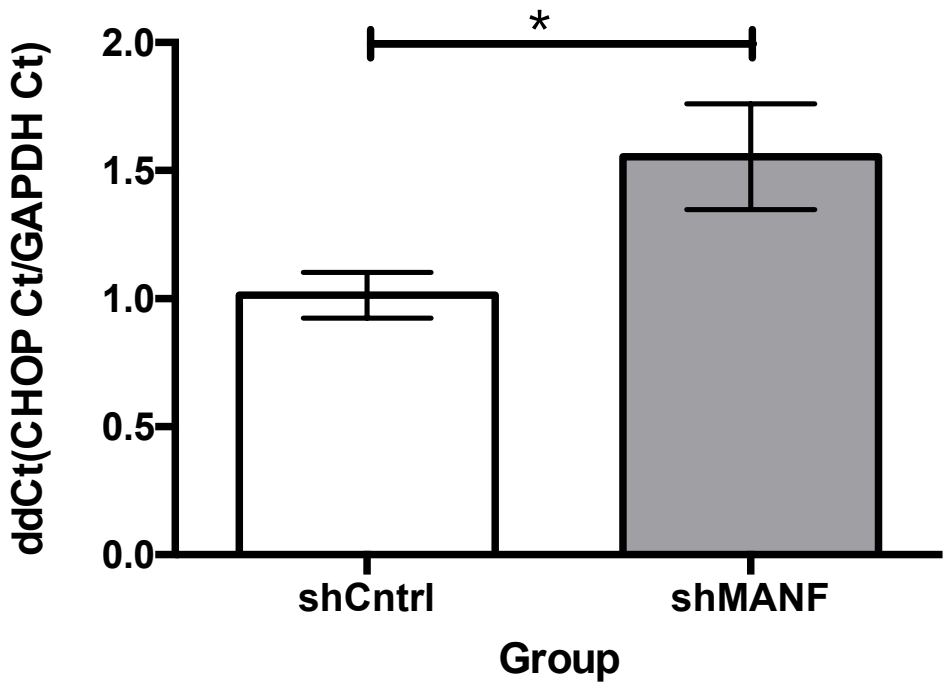

Figure 23: RT-qPCR analysis using the delta-delta Ct method and the unpaired t-test of the apoptotic marker CHOP showed a statistically significant increased expression of CHOP mRNA following lentiviral-mediated shRNA knockdown of MANF in the SN ($p<0.05$)

2.3.7 The effect of Lentiviral-mediated shRNA knockdown of MANF on the mRNA levels of MANF in the striatum and cortex

To confirm that the knockdown of MANF was localized to the SN, mRNA levels of MANF were analyzed in both the striatum and the cortex using RT-qPCR, showing no changes in the level of MANF between both the shMANF group and the shCntrl groups.

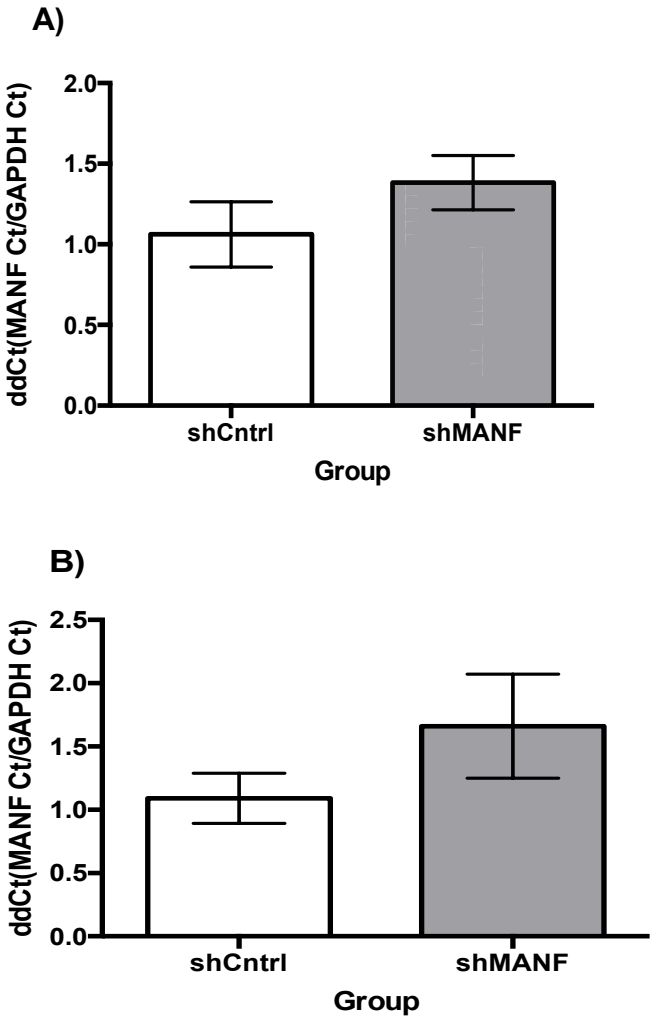

Figure 24: RT-qPCR analysis using the delta-delta Ct method of analysis and the unpaired t-test showed no changes in MANF mRNA levels ($p>0.05$) in either of the (A) Striatum or (B) the cortex

CHAPTER 3- Investigating the neuroprotective effects of curcumin and its effects on MANF expression

3.1 Aims

We aim to establish an in vivo model of PD using 6-OHDA as a toxin and explore curcumin neuroprotective effects and its involvement in ER stress.

1. Study the neuroprotective effects of curcumin against the neurotoxin, 6-OHDA, in an in-vivo model of PD in the mouse striatal cell line and its mediatory effects on MANF.
2. Investigation of the role of curcumin within ER stress
3. Investigation of the pathway through which MANF is upregulated.

3.2 Materials and Methods

3.2.1 STHdh$^{Q7/Q7}$ Neuronal culture

The mouse striatal cell line from a knock in wildtype transgenic mouse with the homozygous huntingtin loci (STHdh$^{Q7/Q7}$) were utilized in this study (Coriell Institute for Medical Research). 80-100% confluency was maintained in adherent cultures in 80% DMEM media, 10% FBS, 1% Geneticin and 1% penicillin/streptomycin solution. Flasks were stored in an incubator at 33^{o} Celsius and were supplemented with 5% CO_2 and 95% O_2. Cells were differentiated 24 hours before any experiment in FBS-free media solution containing 98% DMEM, 1% Geneticin and 1% penicillin/streptomycin solution. Serum starvation increases neurite outgrowth to appropriately resemble striatal models (Figure 23). Following differentiation, STHdh$^{Q7/Q7}$ cells were maintained in FBS-free media.

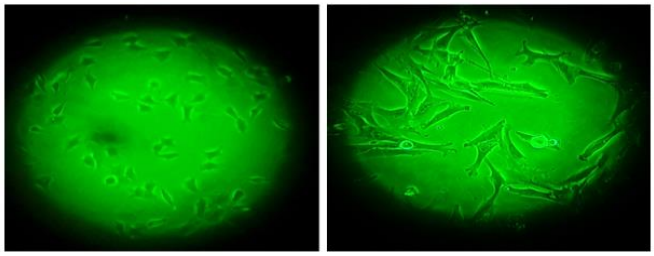

Figure 25: Microscopic image showing neurite outgrowth of the STHdh$^{Q7/Q7}$ neuronal cell culture following differentiation in FBS-free media for 24 hours

3.2.2 Reagent preparation

Curcumin (Sigma, On, Canada cat# C1386) was dissolved in 0.1% DMSO at a concentration of 0.74mg/ml (final concentration of curcumin was 10uM). 6-OHDA (Sigma, On, Canada cat# H4381) was dissolved in 0.2% Ascorbic acid at a concentration of 0.45mg/ml (final concentration of 6-OHDA was 100uM). Ascorbic acid was prepared by dissolving 20mg of Ascorbic acid powder in 10ml of distilled water. The solution's pH was then adjusted to approximately 7.4, and the 6-OHDA powder was added. The 6-OHDA solution was prepared before each experiment, kept in ice, covered in foil and used within the first 30 mins of its preparation to account for 6-OHDA's low stability and to prevent premature oxidation (this form of 6-OHDA has a low to no toxicity in cells). Vehicle control was either 0.1%DMSO, 0.2% Ascorbic acid or a combination of both). Rapamycin was dissolved in 100% methanol at a concentration of 50mg/ml.

3.2.3 Cell density calculation and viability assay

For RNA extraction, cells were plated in a 6-well plate at a density of $6x10^5$ cells/ml (Figure 24). For the viability assay, cells were plated in a 96-well plate at a density of 10,000 cells per well. Cells were counted using 100uL of sample added to 10x diluted

trypan blue solution and cell density was determined on a glass hemocytometer according to the equation below:

$$Cell\ Density\ (\frac{cells}{ml}) = \left[\frac{\left(Average\ of\ 8\ squares\ x\frac{16quadrants}{square}\right)x1.11}{3.2}\right]x1000$$

The neuroprotective effects of curcumin against 6-OHDA was determined by the 3-(4,5-dimethylthiazol-2-yl)-2,5- diphenyltetrazolium bromide (MTT) assay. The MTT assay depends on the mitochondrial metabolic activity of viable cells to assess cell viability (Figure 25). Curcumin was administered as a pretreatment at 10uM for 12 hours and then the media was removed and 6-OHDA was administered at 100uM for 24 hours before cell viability was determined. Control wells contained both the vehicle for curcumin (0.1% DMSO) and for 6-OHDA (0.2 % ascorbic acid).

To assess cell viability, 5mg/ml of Tetrazolim (MTT) powder was dissolved in serum-free media and each well received 20uL of the MTT solution to a total volume of 180uL of media. The plate was incubated for three hours and then the solution was removed from each well. A purple precipitate formed at the bottom of each well, which was then dissolved in 100% DMSO. Fifteen minutes later, absorbance values were obtained using the Spectromax plate reader taken at a wavelength of 570nm. Absorbance values were analyzed in triplicates for each sample and were expressed as percentages of control wells.

For mRNA expression assessment, curcumin was administered at 10uM for 12 hours or as a pretreatment (before 6-OHDA administration) at 10uM for 6 hours to assess effect of curcumin on MANF's expression and on ER stress. The media was then removed and 6-OHDA was administered at 100uM for 12 hours before cells were extracted and

RNA was isolated. Control wells contained both the vehicle for curcumin (0.1% DMSO) and for 6-OHDA (0.2 % ascorbic acid). To assess the effect of mTOR inhibition on MANF mRNA expression, the mTOR blocker Rapamycin was used. Rapamycin was dissolved in 50mg/ml of methanol to a final concentration of 100nM.

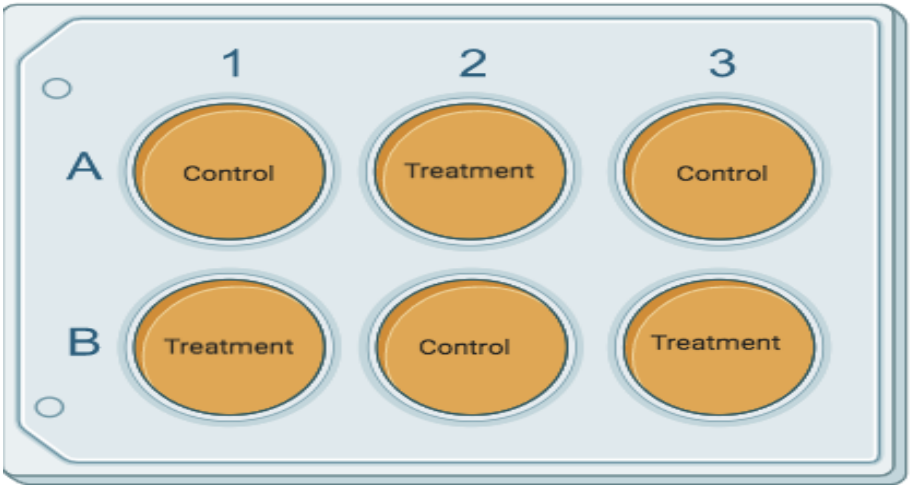

Figure 26: 6-well cell plate setup. Cells were plated in a 6-well plate at a density of $6x10^5$ cells/ml and treatment was administered following 24 hours of differentiation in FBS-free media.

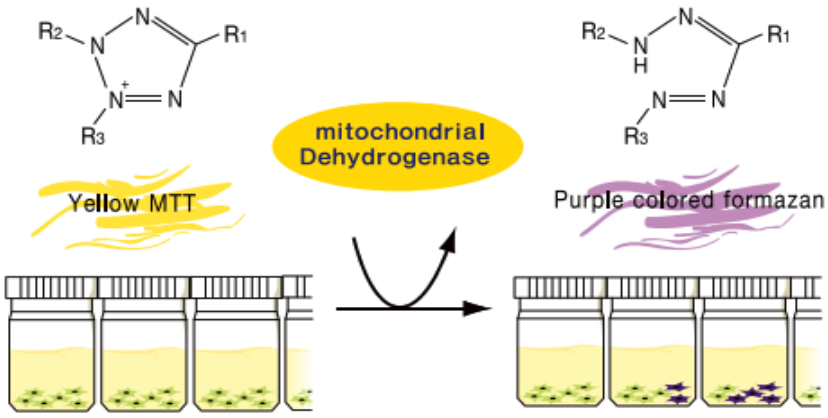

Figure 27: Schematic of the mechanism of MTT assay for cell viability assessment. Viable cells contain intact mitochondria and their mitochondrial dehydrogenase

converts the yellow-colored MTT to purple-colored formazan. A colorimetric assay is then used to determine the percent cell viability.

3.2.4 RNA extraction, cDNA synthesis and RT-qPCR

To extract the cells for mRNA analysis, the media was removed from the wells and 1 ml of serum-free media was added. A cell scraper was used to scrape the cells from the bottom of each well. The media, now containing the cells, is removed and added to a 1.5 ml Eppendorf tube. The tubes are then centrifuged at 7500rpm for 5 minutes. Finally, the media is carefully removed leaving the cells at the bottom the bottom of the tube. Total RNA was extracted via manufacturer's instructions using TRIzol reagent (ThermoFisher Scientific, Catalog#15596018). Cells were first homogenized in 1ml of the TrIzol reagent. Following complete dissolution of the brain tissues, the solution was incubated at room temperature for five minutes. 0.2ml of chloroform was then added to the solution, and it was shaken for 15 seconds. The solution was then centrifuged at 12000g for 15 minutes at 4^{o} Celcius. The colorless RNA phase was then transferred to a 1.5ml eppendorf tube and to the tube 0.5 ml of isopropanol was added. The solution was then shaken for 15 seconds and incubated at room temperature for 10 minutes. Following incubation, the tubes were centrifuged at 12000g for 10 minutes at 4^{o} Celcius. The supernatant was removed and then 1ml of 75% ethanol was added to the RNA pellet. The solution was again centrifuged at maximum speed for 15 minutes at at 4^{o} Celcius. The ethanol was removed and the pellet was allowed to air dry for 10 minutes. The pellet was dissolved in 20uL od DEPC-treated water and heated in a water bath at 60^{o} Celcius for 10 minutes. RNA concentration and purity were determined using the NanoDrop 2000 Spectrophotometer measuring

absorption at 260nm and 280nm. Genomic DNA was removed using the DNAse I enzyme (ThermoFisher Scientific, Catalog#EN0521). The methods for cDNA and RT-qPCR was similar to the methods described in chapter 2. The genes analyzed were mouse MANF, GAPDH, ATF-4 and CHOP (table 2).

Genes	**qPCR primers (5'→3')**
MANF	**Forward:** CGGTTGTGCTACTACATTGGA; **Reverse:** CTGGCTGTCTTCCTTCTTGACC
ATF-4	**Forward:** GCCGGTTTAAGTTGTGTGCT; **Reverse:** CTGGATTCGAGGAATGTGCT
CHOP	**Forward:** CTGCCTTTCACCTTGGAGAC; **Reverse:** CGTTTCCTGGGGATGAGATA
GAPDH	**Forward:** CAACTCCCTCAAGATTGTCAGCAA; **Reverse:** GGCATGGACTGTGGTCATGA

Table 2: Mouse RT-qPCR forward and reverse primer sequences.

3.2.5 Statistics

All statistical analyses were carried out using GraphPad Prism 6.0 software (GraphPad Software, USA). Before analyses, outlier detection was performed using the GraphPad Outlier Tool. One-way ANOVA with Tukey's post-hoc was used as a statistical test to determine difference between multiple groups and results containing only two groups were analyzed using an unpaired Student's t-test. The relative standard curve method and the mRNA copy numbers were used to confirm no differences in the levels of the housekeeping gene GAPDH. In all statistical tests, significance was defined as $*p<0.05$, $**p<0.01$ and $***p<0.001$. Results are presented as plus or minus SEM.

3.3 Results

3.3.1 The effect of Curcumin on SThdh$^{Q7/Q7}$ cell viability

At the beginning of the study, the effects of curcumin on cell viability were assessed to check whether treatment with curcumin induced any cytotoxic effects. Cell viability was assessed using the MTT assay and revealed that following 24 hours of treatment with both 10uM and 50uM of curcumin, no significant changes in cell viability were observed.

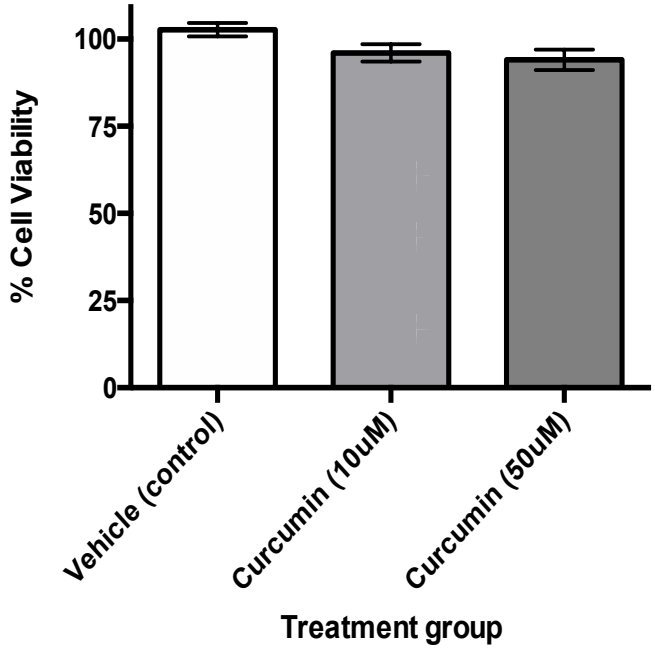

Figure 28: Following cell differentiation, SThdh$^{Q7/Q7}$ cells were treated with either a vehicle control (0.1% DMSO), 10uM Curcumin, or 50uM Curcumin for 24 hours. The effect of the treatment on cell viability was assessed using the MTT assay. At both concentrations Curcumin did not have any statistically significant effect on cell viability.

3.3.2 The effect of 6-OHDA on SThdh$^{Q7/Q7}$ cell viability

The cytotoxic effects of 6-OHDA were analyzed using a cell viability assay following 24 hours of treatment with 6-OHDA at either 50uM or 100uM. Treatment with both concentrations led to a significant reduction in cell viability (ANOVA $p<0.0001$; Tukey test at 50uM, $p<0.0001$; at 100uM, $p<0.001$).

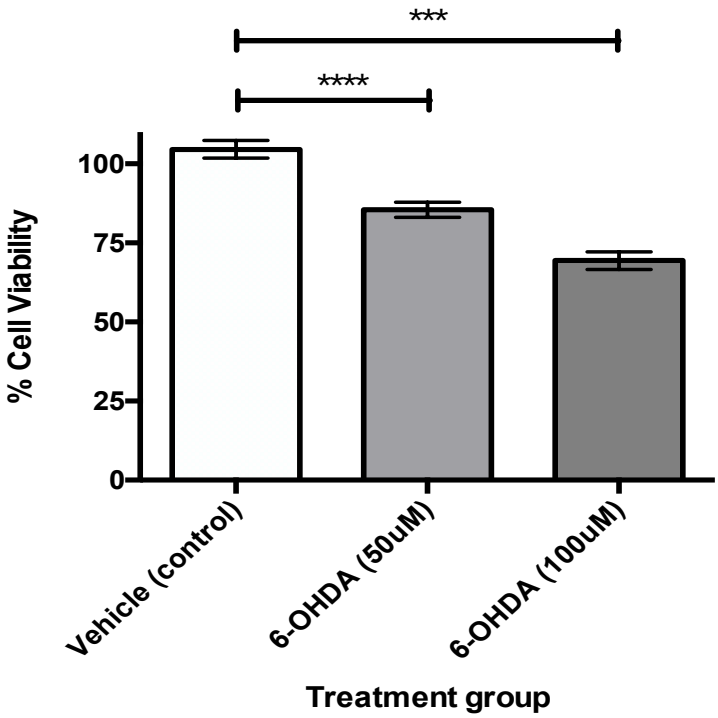

Figure 29: Following cell differentiation, SThdh$^{Q7/Q7}$ cells were treated with either a vehicle control (0.2% Ascorbic acid), 50uM 6-OHDA, or 100uM 6-OHDA for 24 hours. The effect of the treatment on cell viability was assessed using the MTT assay. One-way ANOVA with Tukey's post-hoc showed that both 6-OHDA concentrations caused a statistically significant reduction in cell viability (ANOVA $p<0.0001$; Tukey test at 50uM, $p<0.0001$; at 100uM, $p<0.001$).

3.3.3 The protective effects of Curcumin against 6-OHDA-induced cell death in STHdh$^{Q7/Q7}$

The protective effects of curcumin against 6-OHDA-induced cell death was assessed using the MTT assay. Following differentiation, cells were treated with either a vehicle (both 0.1% DMSO and 0.2% Ascorbic acid), 10uM Curcumin for 24 hours, 100uM 6-OHDA for 24 hours or with 10uM of Curcumin as a pretreatment for 12 hours followed by 100uM 6-OHDA for 24 hours. The introduction of curcumin as a pretreatment to 6-OHDA led to a significant increase in cell viability (ANOVA $p<0.0001$; Tukey test for 6-OHDA $p<0.0001$; Curcumin + 6-OHDA $p<0.05$)

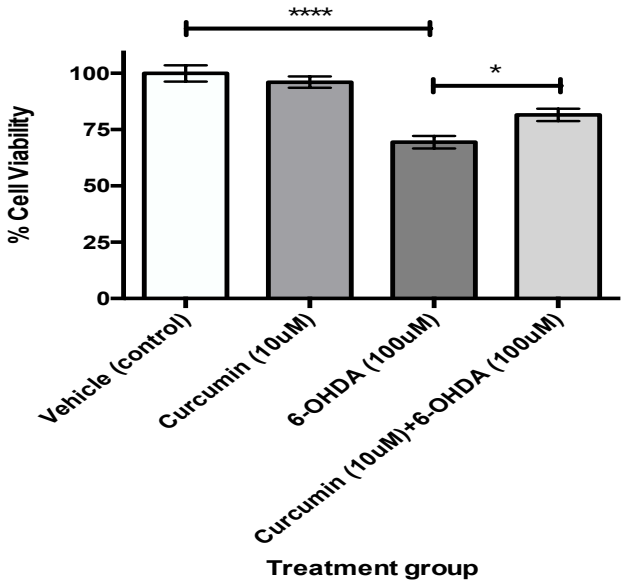

Figure 30: Analysis of cell viability using one-way ANOVA ($p<0.0001$) and Tukey's post-hoc shows that 6-OHDA leads to a statistically significant reduction in cell viability ($p<0.0001$) compared to the control group and a pretreatment with 10uM of curcumin greatly restores and protects cells against the toxic effects of 6-OHDA ($p<0.05$).

3.3.4 The effects of Curcumin on MANF mRNA expression in SThdh$^{Q7/Q7}$

mRNA analysis of the level of MANF were investigated using RT-qPCR following treatment of differentiated SThdh$^{Q7/Q7}$ cells with 10uM of curcumin. Curcumin led to a statistically significant increase in the levels of MANF mRNA ($p<0.01$).

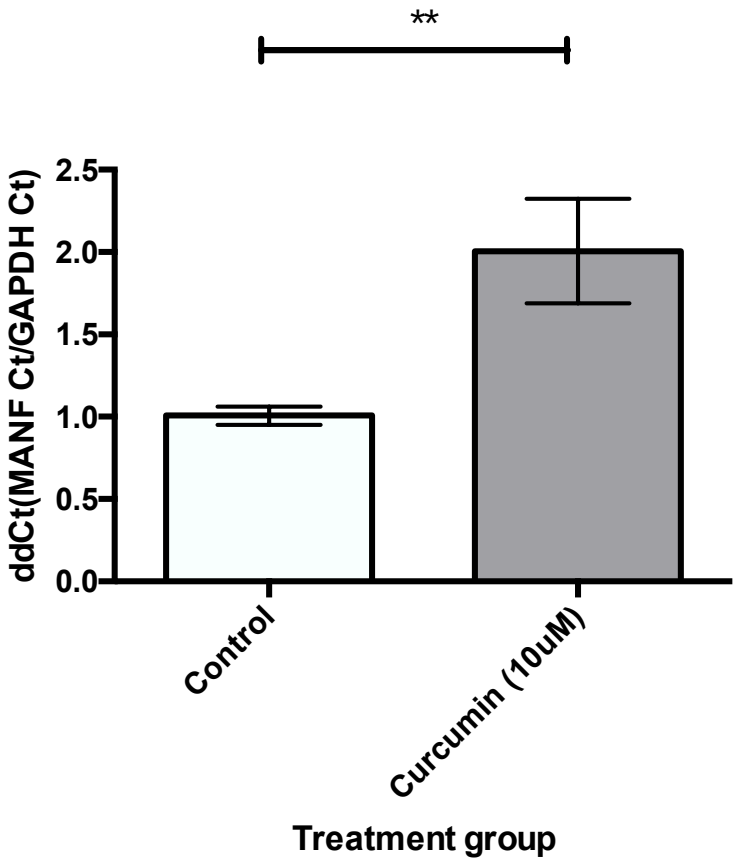

Figure 31: Following differentiation, cells were treated with a vehicle control (0.1% DMSO) and 10uM of Curcumin for 12 hours. RT-qPCR analysis of MANF mRNA using unpaired t-test shows that curcumin administration significantly upregulates MANF's expression relative to control ($p<0.01$).

3.3.5 The effects of Curcumin and 6-OHDA on MANF mRNA expression in STh$dh^{Q7/Q7}$

To investigate curcumin's cytoprotective effects within the 6-OHDA induced cytotoxicity, curcumin was administered as a pretreatment to 6-OHDA for 6-hours. Treatment with 6-OHDA led to a significant decrease in MANF mRNA levels (ANOVA $p<0.0001$, Tukey test $p<0.05$), however, administration of curcumin as a pretreatment to 6-OHDA led to a significant upregulation of MANF mRNA levels ($p<0.01$).

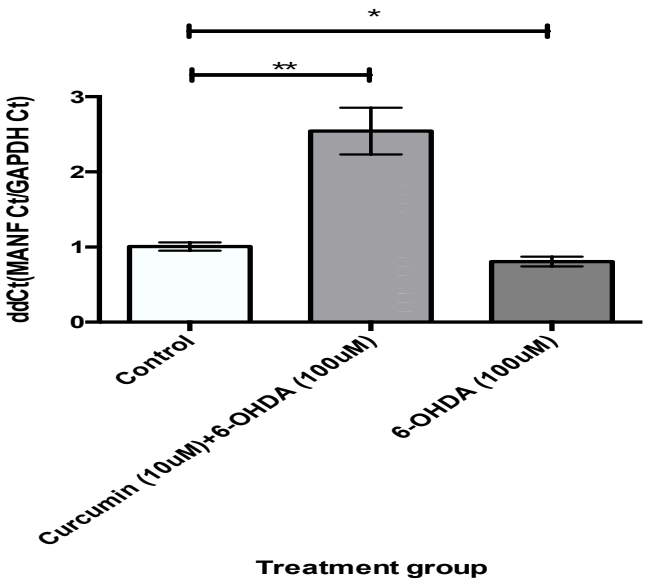

Figure 32: Following differentiation, cells were treated with either a vehicle (both 0.1% DMSO and 0.2% Ascorbic acid), 100uM 6-OHDA for 12 hours or with 10uM of Curcumin as a pretreatment for 6 hours followed by 100uM 6-OHDA for 12 hours. RT-qPCR analysis of MANF mRNA using one-way ANOVA ($p<0.0001$) and Tukey's post-hoc shows that curcumin administration as a pretreatment to 6-OHDA significantly upregulates MANF's expression relative to

control ($p<0.01$). Treatment with 6-OHDA leads to a significant reduction in expression of MANF mRNA ($p<0.05$).

3.3.6 The effects of Curcumin and 6-OHDA on ATF-4 mRNA expression in STHdh$^{Q7/Q7}$

To investigate the effect of curcumin on ER stress, the ER stress marker, ATF-4, was used to assess whether treatment with curcumin would help ameliorate and combat the cell-induced stress that was brought by the neurotoxin 6-OHDA. RT-qPCR analysis of ATF-4 mRNA showed that pretreatment with curcumin significantly reduced ATF-4 mRNA levels (ANOVA $p<0.01$, Tukey test $p<0.01$)

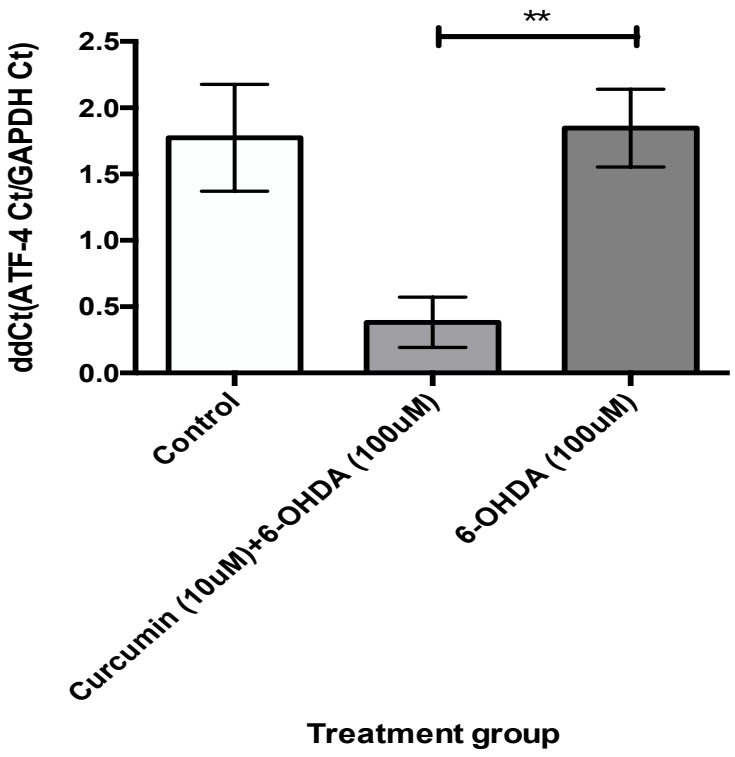

Figure 33: Following differentiation, cells were treated with either a vehicle (both 0.1% DMSO and 0.2% Ascorbic acid), 100uM 6-OHDA for 12 hours or with 10uM of Curcumin as a pretreatment for 6 hours followed by 100uM 6-OHDA for 12 hours. RT-qPCR analysis of ATF-4 mRNA using one-way ANOVA ($p<0.01$) and Tukey's post-hoc shows that curcumin administration significantly downregulates ATF-4 expression relative to 6-OHDA ($p<0.01$).

3.3.7 The effects of Curcumin and 6-OHDA on CHOP mRNA expression in STHdh$^{Q7/Q7}$

To investigate the effect of curcumin on apoptosis, the apoptotic marker, CHOP, was used to assess whether treatment with curcumin would help ameliorate and combat the cell-induced stress that was brought by the neurotoxin 6-OHDA. RT-qPCR analysis of CHOP mRNA showed no significant changes in CHOP mRNA levels.

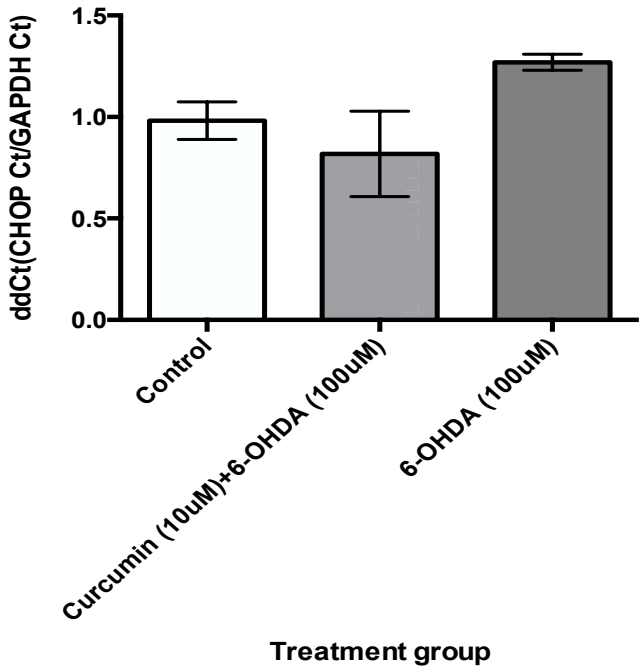

Figure 34: Following differentiation, cells were treated with either a vehicle (both 0.1% DMSO and 0.2% Ascorbic acid), 100uM 6-OHDA for 12 hours or with 10uM of Curcumin as a pretreatment for 6 hours followed by 100uM 6-OHDA for 12 hours. RT-qPCR analysis of CHOP mRNA using one-way ANOVA and Tukey's post-hoc showed no statistically significant difference between the groups.

3.3.8 The effects of Curcumin and Rapamycin on MANF mRNA expression in STHdh$^{Q7/Q7}$

To investigate whether curcumin's upregulation of MANF occurred through the mTOR pathway, STHdh$^{Q7/Q7}$ were co-treated with both the mTOR inhibitor, rapamycin, at 100nM and curcumin at 10uM. MANF mRNA analysis was investigated using RT-qPCR and the results revealed that treatment with rapamycin resulted in a significant upregulation of MANF mRNA and that the co-treated cells also exhibited an upregulation of MANF as opposed to a downregulation (ANOVA $p<0.01$; Tukey test for Curcumin $p<0.01$; Rapamycin $p<0.05$, Curcumin+Rapamycin $p<0.01$).

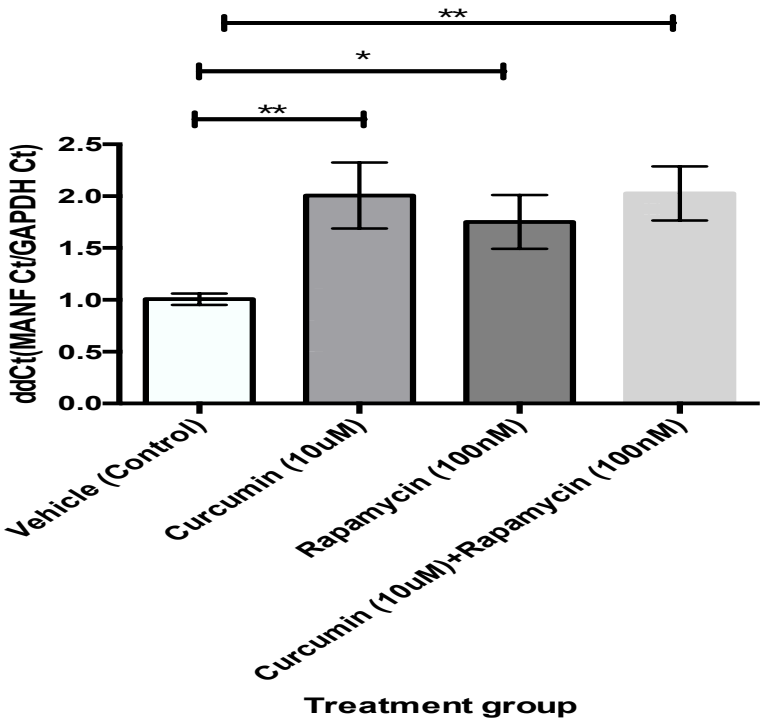

Figure 35: Following differentiation, cells were treated with either a vehicle (both DMSO and methanol), 10uM Curcumin for 12 hours, 100nM Rapamycin for 12 hours or co-treated with 10uM Curcumin and 100nM Rapamycin for 12 hours.

RT-qPCR analysis of MANF mRNA using one-way ANOVA ($p<0.01$) and Tukey's post-hoc that Curcumin significantly upregulated MANF relative to control ($p<0.01$), Rapamycin significantly upregulated MANF relative to control ($p<0.05$) and administration of both Rapamycin and Curcumin significantly upregulated MANF's expression ($p<0.01$).

CHAPTER 4 - Discussion

4.1 The effect of MANF on the pathophysiology of PD

The most important results from this study reveal the significance of MANF as a modulator of the ER stress response and as a neuroprotectant. MANF's lentiviral-mediated shRNA knockdown in the SN has led to the manifestation of motor and gait impairments in rats as well as the induction of the chronic ER stress-UPR axis and the death of DA neurons.

This is the first study of its kind to characterize the long term behavioural deficits and recapitulation of PD-like motor symptoms in rats following the knockdown of MANF and thereby mirroring the chronic nature of PD. The biochemical analysis of the SN has shown that the reduction in the chaperone GRP78 mRNA levels and the upregulation of the apoptotic factor CHOP mRNA levels are indicators of chronic UPR activation and that the apoptotic pathway prevailed. The behavioural deficits are therefore attributed to the loss of dopaminergic neurons within the SN following MANF's knockdown. The levels of MANF in the striatum and cortex were unaffected, implying that the lentiviral-mediated shRNA knockdown was localized within the SN.

The C/EBP homologous protein (CHOP) is a transcription factor that is present at significantly higher levels during ER stress(Samali et al., 2010). During ER stress, PERK mediates the phosphorylation of eIF2α leading to the activation of ATF4 (an ER stress marker), which thereby upregulates CHOP (Samali et al., 2010). During chronic ER stress, the overexpression of CHOP leads to apoptosis through the induction of pro-apoptotic proteins, DR5 (a member of the death-receptor protein family) and depletion of cellular glutathione (leading to an increase in reactive oxygen species) (Samali et al.,

2010). The main apoptotic axis through which CHOP operates is through inducing oxidoreductin-1α (resulting in Hydrogen Peroxide production), which induces the transcription of the ER calcium release channel IP3R1, thereby increasing the release of calcium from the ER and activating apoptosis downstream (Samali et al., 2010). The overexpression of CHOP and the subsequent apoptosis lead to significant implications in many neurodegenerative disorders and CHOP is therefore frequently used as a marker for chronic ER stress and cell death (Samali et al., 2010).

The mechanisms through which MANF operates are still widely unknown and are yet to be elucidated(Lindahl et al., 2017). The ER stress induced apoptosis pathway contributes to the development of neurodegenerative disorder including PD. Our results indicated that the knockdown of MANF lead to a reduction of GRP78 levels, which suggest that MANF's interaction with GRP78 may be essential for the promotion of its protective properties. A study investigating the effects of MANF treatment on two models of PD, including 6-OHDA induced model and an overexpressed alpha-synuclein model in SH-SY5Y cells, revealed that MANF attenuated apoptosis through GRP78 upregulation and a reduction of activated caspase levels(Huang et al., 2016).

Multiple studies have pointed to the importance of GRP78's protective properties and its relevance in neurodegenerative disease progression(Lew, 2007; Shen, Chen, Hendershot, & Prywes, 2002). GRP78's levels were found to reduce with age, which explains the susceptibility of older mice to age-related neurodegenerative disorders(Shen et al., 2002). There are studies that demonstrate GRP78 elevation in ER stress induced models and lower levels in MANF-treated groups(Yang et al., 2014). This may be

explained by the fact that GRP78 is involved in the survival mechanism and therefore the induction of stressed states may basally activate GRP78 in a compensatory fashion. However, these compensatory mechanisms may have a limited therapeutic effect such as within the 6-OHDA model(Huang et al., 2016). These results may therefore be explained by MANF acting in a protective fashion to attenuate the stressors, and, in a time-dependent manner, may act as a negative regulator of GRP78 in a feedback loop, following stress elimination(Huang et al., 2016).

MANF's role within ER stress has been widely studied in multiple systems. MANF has proven to be protective against cerebral ischemia shown by a decrease in the volume of infarction in adult rats and also by a decrease in locomotor asymmetry as well as a decrease in cell death when MANF was administered as a pretreatment(Airavaara et al., 2010). Mice knockout models of MANF have shown to exhibit insulin-dependent diabetes as a result of beta-islets of Langerhans loss in the pancreas as a result of elevated ER stress and apoptosis(Lindahl et al., 2014). MANF has also been shown to act as a cardiomykine, which are heart-derived proteins that act to regulate cardiovascular function(Glembotski, 2011). Myocardial injury leads to the activation of the ER stress and UPR axis and MANF has proven to be an effective attenuator of the response thereby promoting protective anti-hypertrophic activities(Glembotski, 2011). Moreover, pretreatment of 6-OHDA PD rat models with MANF has proven to promote the survival of about 80% of DA neurons(Merja H. Voutilainen et al., 2015).

4.2 The neuroprotective effects of curcumin

Our results demonstrated curcumin's significant anti-oxidant properties and its ability to modulate its therapeutic effect through upregulation of the MANF. Curcumin acts as a scavenger against ROS due to its various functional groups.

Within the context of PD, curcumin has demonstrated protective effects in 6-hydroxydopamine (6-OHDA) model of PD, by improving striatal DA levels. Treatment with 6-OHDA led to a significant reduction in cell viability of about 65-70%. However, pretreatment with curcumin was shown to improve cell viability and maintain it at around 85%. This is attributed to curcumin's phenolic groups that act as electron traps, thereby preventing the formation of ROS such as H_2O_2 and superoxide (SHISHODIA, 2005). Curcumin has shown to also prevent alpha-synuclein protein aggregation in vitro by enhancing the protein's solubility and attenuating its toxic effects. This activity is facilitated by the methylenic and the phenolic groups of curcumin(Sharma & Nehru, 2018). Curcumin has demonstrated to be protective against mitochondrial nitosylation and nitration induced by ROS in neurons, and therefore prevented apoptosis of these cells(Kao, Hu, Wu, & Kong, 2016).

Moreover, our results are consistent with studies showing the effect of curcumin on the ER stress pathway and its ability to attenuate ATF-4 activation, thereby halting the apoptotic axis and improving cell viability. Treatment with 6-OHDA did not show any significant upregulation of either ATF-4 or CHOP mRNA and this might be due to the fact that the treatment was only administered for 12-hours, which might not be sufficient time to induce any phenotypic changes in cell viability downstream. However, it is well

established that both ATF-4 and CHOP are significantly upregulated in 6-OHDA-induced cytotoxicity (Y. Zhang et al., 2017). Due to the low sample size and the failure of our results in to demonstrate 6-OHDA's cytotoxicity molecularly, replication of the experiment is warranted with a longer incubation period to accurately model the changes in the ER-stress and apoptotic axis.

We hypothesized that MANF's upregulation may be mediated through the PI3k/AKT/mTOR pathway. However, co-treatment of STHdh$^{Q7/Q7}$ cells with both the mTORC1 blocker, Rapamycin, as well as Curcumin did not prevent the Curcumin-induced upregulation of MANF. Moreover, Rapamycin was seen to upregulate MANF's expression and hence the results were contradictory to what was originally hypothesized. These findings can be interpreted by assessing the nature of MANF's upregulation, which has proven to be induced during ER stress conditions. Therefore, an alternative hypothesis would be that Rapamycin, through mTORC1 inhibition, induces cellular stress and because MANF is ER stress inducible protein, its levels were increased as a result of UPR activation.

This pathway might be distinct from the pathway through which curcumin upregulates MANF, due to the fact that curcumin is an attenuator of ER stress and hence might not upregulate MANF through an ER stress induced response. In that case, an additive effect should have also been seen with MANF's expression when both curcumin and rapamycin, however treatment with curcumin showed similar levels of MANF's expression, with and without treatment with rapamycin (Figure 35). This therefore justifies the investigation of the ER stress response following treatment with rapamycin

and replication of our experiment to assess any additive effect on MANF's expression that might be incurred when rapamycin is administered.

4.3 Conclusion and future directions

Our results strongly support curcumin's neuroprotective properties and show that MANF is one the neuroprotective agents employed. Moreover, curcumin's downregulation of the ER stress pathway through ATF-4 downregulation further elucidates its capability to prevent the stress-induced death caused by 6-OHDA. We failed however to show the pathway through which MANF was upregulated. Furthermore, although there is a plethora of evidence that clearly point towards MANF's protective properties and there are many theories put in place to describe MANF's specific mechanism, there hasn't been any definitive evidence to suggest how exactly MANF behaves to combat cell stressors and promote its survival(Lindahl et al., 2017). Identifying MANF's cellular receptors would provide us with a great starting point.

The peroxisome proliferator-activated receptors (PPARs) represent a family of nuclear receptor proteins and act as transcription factors that regulate gene expression(Berger & Moller, 2002). PPAR-gamma is the most widely studied PPAR due to its therapeutic capacity in a wide variety of metabolic disorders. PPAR-gamma receptors influence gene expression through binding to DNA sequences known as peroxisome proliferator response elements (PPRE)(Z.-J. Liu et al., 2013).

Within the context of PD, the PPAR-gamma receptor was shown to protect neurons against oxidative stress mainly through inhibition of the NF-xB pathway(Victor et al., 2006). Curcumin demonstrated to be an effective PPAR-gamma agonist and was

capable of promoting the survival of neurons(Z.-J. Liu et al., 2013). It was concluded that curcumin may thereby contribute its neuroprotective properties through its mediatory effects on PPAR-gamma(Z.-J. Liu et al., 2013). Therefore, the PPAR-gamma pathway would be worth investigation in the future to outline the mechanism through which curcumin modulates the levels of MANF.

To sum up, this study, in addition to the existing body of knowledge, acknowledges MANF's role within the ER stress pathway pointing to its critical neuroprotective properties and warrant extensive investigation of its mechanistic properties due to the considerable potential that it withholds as a therapeutic. The failure of GDNF in clinical trials as well as MANF's unique properties and its current supporting evidence are stimulators for investigation of MANF's success in clinical trials. Future models should also investigate MANF's neuro-restorative properties in well-established models of PD such as 6-OHDA and MPTP models. Moreover, the protective and anti-oxidant effects of curcumin and its ability to attenuate induced cytotoxic states, in addition to its low toxicity justify paves the way for the investigation of its specific mechanistic roles and use as a neuroprotectant.

*All published figures have been reused with permission from the publisher.

References:

Aggarwal, B. B., & Harikumar, K. B. (2009). Potential therapeutic effects of curcumin, the anti-inflammatory agent, against neurodegenerative, cardiovascular, pulmonary, metabolic, autoimmune and neoplastic diseases. *The International Journal of Biochemistry & Cell Biology*, *41*(1), 40–59. https://doi.org/10.1016/j.biocel.2008.06.010

Agid, Y. (1991). Parkinson's disease: pathophysiology. *The Lancet*, *337*(8753), 1321–1324. https://doi.org/10.1016/0140-6736(91)92989-F

Airavaara, M., Chiocco, M. J., Howard, D. B., Zuchowski, K. L., Peränen, J., Liu, C., … Harvey, B. K. (2010). Widespread cortical expression of MANF by AAV serotype 7: Localization and protection against ischemic brain injury. *Experimental Neurology*, *225*(1), 104–113. https://doi.org/10.1016/j.expneurol.2010.05.020

Berger, J., & Moller, D. E. (2002). The Mechanisms of Action of PPARs. *Annual Review of Medicine*, *53*(1), 409–435. https://doi.org/10.1146/annurev.med.53.082901.104018

Blandini, F., Nappi, G., Tassorelli, C., & Martignoni, E. (2000). Functional changes of the basal ganglia circuitry in Parkinson's disease. *Progress in Neurobiology*, *62*(1), 63–88. https://doi.org/10.1016/S0301-0082(99)00067-2

Blesa, J., & Przedborski, S. (2014). Parkinsonâ€™s disease: animal models and dopaminergic cell vulnerability. *Frontiers in Neuroanatomy*, *8*. https://doi.org/10.3389/fnana.2014.00155

Blesa, J., Trigo-Damas, I., Quiroga-Varela, A., & Jackson-Lewis, V. R. (2015). Oxidative

stress and Parkinson's disease. *Frontiers in Neuroanatomy*, *9*, 91. https://doi.org/10.3389/fnana.2015.00091

Brooks, S. P., & Dunnett, S. B. (2009). Tests to assess motor phenotype in mice: a user's guide. *Nature Reviews Neuroscience*, *10*(7), 519–529. https://doi.org/10.1038/nrn2652

Danilova, T., & Lindahl, M. (2018). Emerging Roles for Mesencephalic Astrocyte-Derived Neurotrophic Factor (MANF) in Pancreatic Beta Cells and Diabetes. *Frontiers in Physiology*, *9*, 1457. https://doi.org/10.3389/fphys.2018.01457

Dauer, W., & Przedborski, S. (2003). Parkinson's Disease. *Neuron*, *39*(6), 889–909. https://doi.org/10.1016/S0896-6273(03)00568-3

Deumens, R., Blokland, A., & Prickaerts, J. (2002). Modeling Parkinson's Disease in Rats: An Evaluation of 6-OHDA Lesions of the Nigrostriatal Pathway. *Experimental Neurology*, *175*(2), 303–317. https://doi.org/10.1006/exnr.2002.7891

Dhillon, N., Aggarwal, B. B., Newman, R. A., Wolff, R. A., Kunnumakkara, A. B., Abbruzzese, J. L., … Kurzrock, R. (2008). Phase II Trial of Curcumin in Patients with Advanced Pancreatic Cancer. *Clinical Cancer Research*, *14*(14), 4491–4499. https://doi.org/10.1158/1078-0432.CCR-08-0024

Glembotski, C. C. (2011). Functions for the cardiomyokine, MANF, in cardioprotection, hypertrophy and heart failure. *Journal of Molecular and Cellular Cardiology*, *51*(4), 512–517. https://doi.org/10.1016/j.yjmcc.2010.10.008

Hao, F., Yang, C., Chen, S.-S., Wang, Y.-Y., Zhou, W., Hao, Q., … Xu, Q.-Y. (2017). Long-term protective effects of AAV9-mesencephalic astrocyte-derived

neurotrophic factor gene transfer in parkinsonian rats. *Experimental Neurology*, *291*, 120–133. https://doi.org/10.1016/j.expneurol.2017.01.008

Hirsch, L., Jette, N., Frolkis, A., Steeves, T., & Pringsheim, T. (2016). The Incidence of Parkinson's Disease: A Systematic Review and Meta-Analysis. *Neuroepidemiology*, *46*(4), 292–300. https://doi.org/10.1159/000445751

Huang, J., Chen, C., Gu, H., Li, C., Fu, X., Jiang, M., … Jin, L. (2016). Mesencephalic astrocyte-derived neurotrophic factor reduces cell apoptosis via upregulating GRP78 in SH-SY5Y cells. *Cell Biology International*, *40*(7), 803–811. https://doi.org/10.1002/cbin.10621

Huse, D. M., Schulman, K., Orsini, L., Castelli-Haley, J., Kennedy, S., & Lenhart, G. (2005). Burden of illness in Parkinson's disease. *Movement Disorders*, *20*(11), 1449–1454. https://doi.org/10.1002/mds.20609

Jenner, P. (2003). Oxidative stress in Parkinson's disease. *Annals of Neurology*, *53*(S3), S26–S38. https://doi.org/10.1002/ana.10483

Kao, N.-J., Hu, J.-Y., Wu, C.-S., & Kong, Z.-L. (2016). Curcumin represses the activity of inhibitor-κB kinase in dextran sulfate sodium-induced colitis by S-nitrosylation. *International Immunopharmacology*, *38*, 1–7. https://doi.org/10.1016/j.intimp.2016.05.015

Kordower, J. H., & Bjorklund, A. (2013). Trophic Factor Gene Therapy for Parkinson's Disease. *Movement Disorders*, *28*(1), 96–109. https://doi.org/10.1002/mds.25344

Laplante, M., & Sabatini, D. M. (2009). mTOR signaling at a glance. *Journal of Cell Science*, *122*(20), 3589–3594. https://doi.org/10.1242/jcs.051011

Lew, M. (2007). Overview of Parkinson's Disease. *Journal of the American Medical Directors Association*, *6*(4), 4–16. https://doi.org/10.1016/j.jamda.2005.07.005

LeWitt, P. A. (2008). Levodopa for the Treatment of Parkinson's Disease. *New England Journal of Medicine*, *359*(23), 2468–2476. https://doi.org/10.1056/NEJMct0800326

Lindahl, M., Danilova, T., Palm, E., Lindholm, P., Võikar, V., Hakonen, E., … Saarma, M. (2014). MANF Is Indispensable for the Proliferation and Survival of Pancreatic β Cells. *Cell Reports*, *7*(2), 366–375. https://doi.org/10.1016/j.celrep.2014.03.023

Lindahl, M., Saarma, M., & Lindholm, P. (2017). Unconventional neurotrophic factors CDNF and MANF: Structure, physiological functions and therapeutic potential. *Neurobiology of Disease*, *97*, 90–102. https://doi.org/10.1016/j.nbd.2016.07.009

Liu, H., Tang, X., & Gong, L. (2015). Mesencephalic astrocyte-derived neurotrophic factor and cerebral dopamine neurotrophic factor: New endoplasmic reticulum stress response proteins. *European Journal of Pharmacology*, *750*, 118–122. https://doi.org/10.1016/j.ejphar.2015.01.016

Liu, Z.-J., Liu, W., Liu, L., Xiao, C., Wang, Y., & Jiao, J.-S. (2013). Curcumin Protects Neuron against Cerebral Ischemia-Induced Inflammation through Improving PPAR-Gamma Function. *Evidence-Based Complementary and Alternative Medicine*, *2013*, 1–10. https://doi.org/10.1155/2013/470975

Mythri, R. B., & Bharath, M. M. S. (2012). Curcumin: a potential neuroprotective agent in Parkinson's disease. *Current Pharmaceutical Design*, *18*(1), 91–99. Retrieved from http://www.ncbi.nlm.nih.gov/pubmed/22211691

Petrova, P., Raibekas, A., Pevsner, J., Vigo, N., Anafi, M., Moore, M. K., …

Commissiong, J. W. (2003). MANF: a new mesencephalic, astrocyte-derived neurotrophic factor with selectivity for dopaminergic neurons. *Journal of Molecular Neuroscience : MN*, *20*(2), 173–188. Retrieved from http://www.ncbi.nlm.nih.gov/pubmed/12794311

Samali, A., FitzGerald, U., Deegan, S., & Gupta, S. (2010). Methods for Monitoring Endoplasmic Reticulum Stress and the Unfolded Protein Response. *International Journal of Cell Biology*, *2010*, 1–11. https://doi.org/10.1155/2010/830307

Santel, T., Pflug, G., Hemdan, N. Y. A., Schäfer, A., Hollenbach, M., Buchold, M., … Birkenmeier, G. (2008). Curcumin Inhibits Glyoxalase 1—A Possible Link to Its Anti-Inflammatory and Anti-Tumor Activity. *PLoS ONE*, *3*(10), e3508. https://doi.org/10.1371/journal.pone.0003508

Sharma, N., & Nehru, B. (2018). Curcumin affords neuroprotection and inhibits α-synuclein aggregation in lipopolysaccharide-induced Parkinson's disease model. *Inflammopharmacology*, *26*(2), 349–360. https://doi.org/10.1007/s10787-017-0402-8

Shen, J., Chen, X., Hendershot, L., & Prywes, R. (2002). ER stress regulation of ATF6 localization by dissociation of BiP/GRP78 binding and unmasking of Golgi localization signals. *Developmental Cell*, *3*(1), 99–111. Retrieved from https://www.sciencedirect.com/science/article/pii/S1534580702002034

SHISHODIA, S. (2005). Curcumin: Getting Back to the Roots. *Annals of the New York Academy of Sciences*, *1056*(1), 206–217. https://doi.org/10.1196/annals.1352.010

Shulman, J. M., De Jager, P. L., & Feany, M. B. (2011). Parkinson's Disease: Genetics

and Pathogenesis. *Annual Review of Pathology: Mechanisms of Disease*, *6*(1), 193–222. https://doi.org/10.1146/annurev-pathol-011110-130242

Spillantini, M. G., Schmidt, M. L., Lee, V. M.-Y., Trojanowski, J. Q., Jakes, R., & Goedert, M. (1997). α-Synuclein in Lewy bodies. *Nature*, *388*(6645), 839–840. https://doi.org/10.1038/42166

Tomita, M., Holman, B. J., Santoro, C. P., & Santoro, T. J. (2005). Astrocyte production of the chemokine macrophage inflammatory protein-2 is inhibited by the spice principle curcumin at the level of gene transcription. *Journal of Neuroinflammation*, *2*(1), 8. https://doi.org/10.1186/1742-2094-2-8

Van den Haute, C., Eggermont, K., Nuttin, B., Debyser, Z., & Baekelandt, V. (2003). Lentiviral Vector-Mediated Delivery of Short Hairpin RNA Results in Persistent Knockdown of Gene Expression in Mouse Brain. *Human Gene Therapy*, *14*(18), 1799–1807. https://doi.org/10.1089/104303403322611809

Victor, N. A., Wanderi, E. W., Gamboa, J., Zhao, X., Aronowski, J., Deininger, K., … Sundararajan, S. (2006). Altered PPARγ expression and activation after transient focal ischemia in rats. *European Journal of Neuroscience*, *24*(6), 1653–1663. https://doi.org/10.1111/j.1460-9568.2006.05037.x

Voutilainen, M. H., Back, S., Porsti, E., Toppinen, L., Lindgren, L., Lindholm, P., … Tuominen, R. K. (2009a). Mesencephalic Astrocyte-Derived Neurotrophic Factor Is Neurorestorative in Rat Model of Parkinson's Disease. *Journal of Neuroscience*, *29*(30), 9651–9659. https://doi.org/10.1523/JNEUROSCI.0833-09.2009

Voutilainen, M. H., Back, S., Porsti, E., Toppinen, L., Lindgren, L., Lindholm, P., …

Tuominen, R. K. (2009b). Mesencephalic Astrocyte-Derived Neurotrophic Factor Is Neurorestorative in Rat Model of Parkinson's Disease. *Journal of Neuroscience*, *29*(30), 9651–9659. https://doi.org/10.1523/JNEUROSCI.0833-09.2009

Voutilainen, Merja H., Arumäe, U., Airavaara, M., & Saarma, M. (2015). Therapeutic potential of the endoplasmic reticulum located and secreted CDNF/MANF family of neurotrophic factors in Parkinson's disease. *FEBS Letters*, *589*(24PartA), 3739–3748. https://doi.org/10.1016/j.febslet.2015.09.031

Wang, J., Du, X.-X., Jiang, H., & Xie, J.-X. (2009). Curcumin attenuates 6-hydroxydopamine-induced cytotoxicity by anti-oxidation and nuclear factor-kappaB modulation in MES23.5 cells. *Biochemical Pharmacology*, *78*(2), 178–183. https://doi.org/10.1016/j.bcp.2009.03.031

Wang, S.-F., Liu, L.-F., Wu, M.-Y., Cai, C.-Z., Su, H., Tan, J., … Li, M. (2017). Baicalein prevents 6-OHDA/ascorbic acid-induced calcium-dependent dopaminergic neuronal cell death. *Scientific Reports*, *7*(1), 8398. https://doi.org/10.1038/s41598-017-07142-7

Williams, B. L., & Lipkin, W. I. (2006). Endoplasmic reticulum stress and neurodegeneration in rats neonatally infected with borna disease virus. *Journal of Virology*, *80*(17), 8613–8626. https://doi.org/10.1128/JVI.00836-06

Wong, S. L., Gilmour, H., & Ramage-Morin, P. L. (2014). Parkinson's disease: Prevalence, diagnosis and impact. *Health Reports*, *25*(11), 10–14. Retrieved from http://www.ncbi.nlm.nih.gov/pubmed/25408491

Yang, W., Shen, Y., Chen, Y., Chen, L., Wang, L., Wang, H., … Shen, Y. (2014).

Mesencephalic astrocyte-derived neurotrophic factor prevents neuron loss via inhibiting ischemia-induced apoptosis. *Journal of the Neurological Sciences*, *344*(1–2), 129–138. https://doi.org/10.1016/j.jns.2014.06.042

Zhang, Y., Long, H., Zhou, F., Zhu, W., Ruan, J., Zhao, Y., & Lu, Y. (2017). Echinacoside's nigrostriatal dopaminergic protection against 6-OHDA-Induced endoplasmic reticulum stress through reducing the accumulation of Seipin. *Journal of Cellular and Molecular Medicine*, *21*(12), 3761–3775. https://doi.org/10.1111/jcmm.13285

Zhang, Z., Shen, Y., Luo, H., Zhang, F., Peng, D., Jing, L., … Jin, L. (2018). MANF protects dopamine neurons and locomotion defects from a human α-synuclein induced Parkinson's disease model in C. elegans by regulating ER stress and autophagy pathways. *Experimental Neurology*, *308*, 59–71. https://doi.org/10.1016/j.expneurol.2018.06.016